UNIVERSIDADE FEDERAL DO PARANÁ

MARCO AURÉLIO CAMARGO FONTANELA

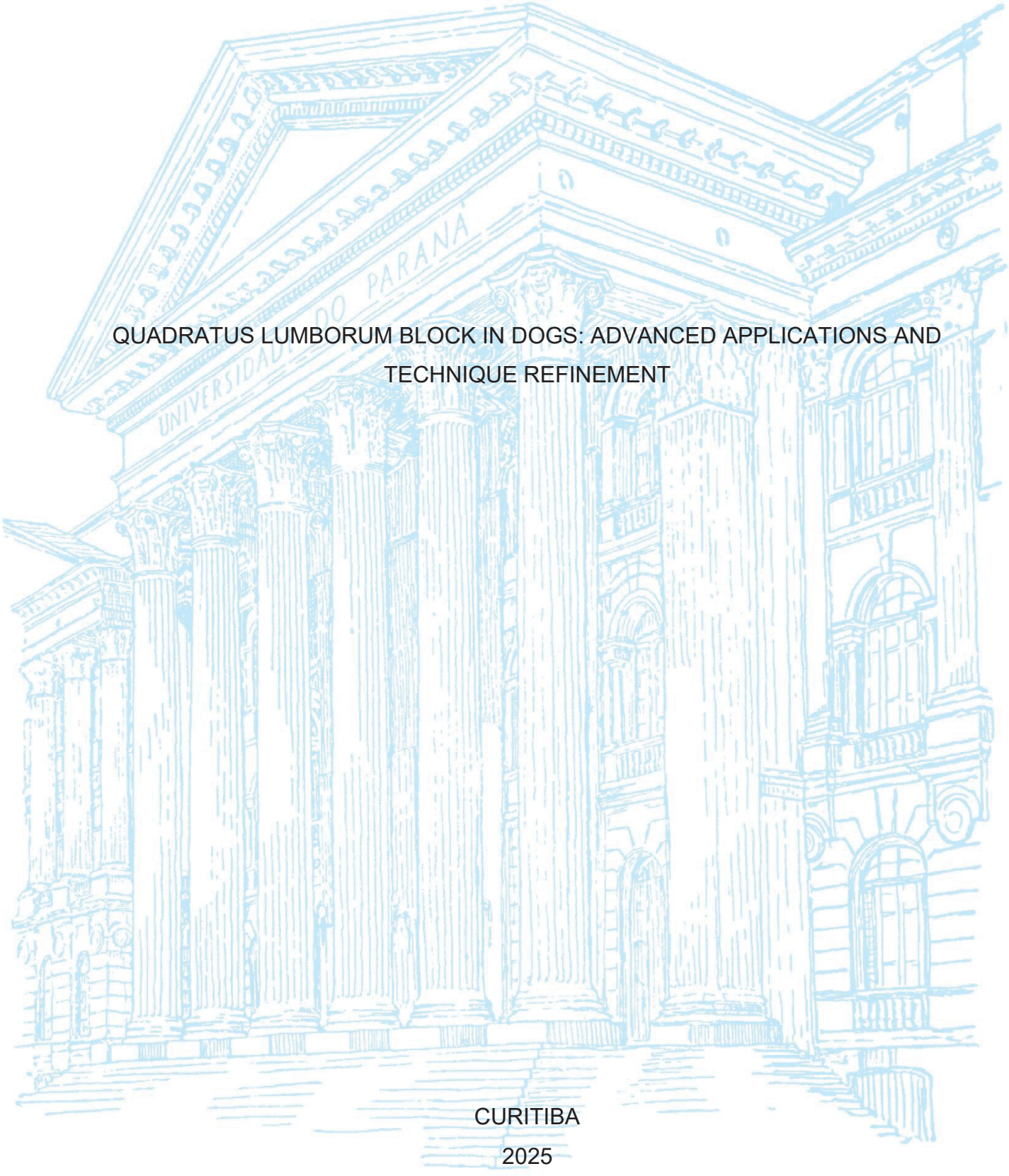

QUADRATUS LUMBORUM BLOCK IN DOGS: ADVANCED APPLICATIONS AND TECHNIQUE REFINEMENT

CURITIBA

2025

MARCO AURÉLIO CAMARGO FONTANELA

QUADRATUS LUMBORUM BLOCK IN DOGS: ADVANCED APPLICATIONS AND TECHNIQUE REFINEMENT

Tese apresentada ao Programa de Pós-Graduação em Ciências Veterinárias, Setor de Ciências Agrárias, da Universidade Federal do Paraná, como requisito parcial para obtenção do título de Doutor em Ciências Veterinárias.

Orientador. Prof. Dr. Juan Carlos Duque Moreno

CURITIBA
2025

DADOS INTERNACIONAIS DE CATALOGAÇÃO NA PUBLICAÇÃO (CIP)
UNIVERSIDADE FEDERAL DO PARANÁ
SISTEMA DE BIBLIOTECAS – BIBLIOTECA DE CIÊNCIAS AGRÁRIAS

Fontanela, Marco Aurélio Camargo
Quadratus lumborum block in dogs: advanced applications and technique refinement / Marco Aurélio Camargo Fontanela. – Curitiba, 2025.
1 recurso online: PDF.

Tese (Doutorado) – Universidade Federal do Paraná, Setor de Ciências Agrárias, Programa de Pós-Graduação em Ciências Veterinárias.
Orientador: Prof. Dr. Juan Carlos Duque Moreno

1. Cães. 2. Cirurgia veterinária. 3. Anestesia por condução. 4. Peritonite. I. Moreno, Juan Carlos Duque. II. Universidade Federal do Paraná. Programa de Pós-Graduação em Ciências Veterinárias. III. Título.

Bibliotecária: Ana Camila Quaresma Moura CRB-9/2212

TERMO DE APROVAÇÃO

Os membros da Banca Examinadora designada pelo Colegiado do Programa de Pós-Graduação CIÊNCIAS VETERINÁRIAS da Universidade Federal do Paraná foram convocados para realizar a arguição da tese de Doutorado de **MARCO AURELIO CAMARGO FONTANELA**, intitulada: **QUADRATUS LUMBORUM BLOCK IN DOGS: ADVANCED APPLICATIONS AND TECHNIQUE REFINEMENT**, sob orientação do Prof. Dr. JUAN CARLOS DUQUE MORENO, que após terem inquirido o aluno e realizada a avaliação do trabalho, são de parecer pela sua aprovação no rito de defesa.

A outorga do título de doutor está sujeita à homologação pelo colegiado, ao atendimento de todas as indicações e correções solicitadas pela banca e ao pleno atendimento das demandas regimentais do Programa de Pós-Graduação.

CURITIBA, 28 de Fevereiro de 2025.

Documento assinado digitalmente
gov.br
JUAN CARLOS DUQUE MORENO
Data: 11/04/2025 08:46:33-0300
Verifique em https://validar.iti.gov.br

JUAN CARLOS DUQUE MORENO
Presidente da Banca Examinadora

Documento assinado digitalmente
gov.br
MARCELLO MACHADO
Data: 10/04/2025 20:21:45-0300
Verifique em https://validar.iti.gov.br

MARCELLO MACHADO
Avaliador Externo (DEPTO DE ANATOMIA - UFPR)

Documento assinado digitalmente
gov.br
PAULO ROBERTO KLAUMANN
Data: 10/04/2025 08:18:30-0300
Verifique em https://validar.iti.gov.br

PAULO ROBERTO KLAUMANN
Avaliador Externo (ANESTESIOLOGIA VETERINÁRIA)

JAIME VISCASILLAS MONTEAGUDO
Avaliador Externo (ANICURA VALENCIA SUR HOSPITAL VETERINARIO)

Documento assinado digitalmente
gov.br
PETERSON TRICHES DORNBUSCH
Data: 12/04/2025 08:20:41-0300
Verifique em https://validar.iti.gov.br

PETERSON TRICHES DORNBUSCH
Avaliador Interno (UNIVERSIDADE FEDERAL DO PARANÁ)

Dedico esse trabalho a minha avó Benta do Carmo Nunes, que me proporcionou uma infância confortável, e a minha mãe Francisca Julia Camargo Dresch, que me motivou e me proporcionou estudo de qualidade.

AGRADECIMENTOS

Ao meu orientador Juan Carlos Duque, que direcionou e corrigiu esta tese, além de ter sido capaz de promover um cuidado e preocupação além do acadêmico (mesmo que do seu jeito).

A minha companheira Karina Silva dos Santos, que esteve do meu lado e me ajudou nos momentos importantes, deixando a caminhada mais agradável.

Ao meu pai Edmilson Fontanela, que me proporcionou a compra de equipamentos necessários para conseguir me manter em Curitiba e que me fez pensar com nossas conversas sobre o futuro.

Ao meu patrão Sylvio Elias, que me contratou em um momento difícil, me proporcionou cuidados de um pai e sempre me ajudou em absolutamente todas as minhas necessidades.

Ao professor Marcello Machado, que tem um amor enorme em ensinar anatomia e sempre esteve presente nos meu pedidos de ajuda.

A minha ex-orientadora Marilda Onghero Taffarel, que mantemos amizade para a vida e trocas acadêmicas importantes.

Ao veterinário anestesista José Kloss, que me ajudou muito nos últimos meses desse período e realmente manteve uma equipe.

Aos meus colegas de pós-graduação e/ou participantes dos projetos: Marina Moresco, Guilherme Lopes, Gilberto Serighelli, Viviane Bosak, Eloisa Melbauher, Mariana Rodrigues, Julia Franco, Priscila Ferreira, Robson Piontkovski e Iara Luiza Matos de Lima.

Ao Laboratório de Patologia Clínica do Hospital Veteináiro, Setor de Ciências Agrárias da UFPR, seus colaboradores e em especial à professora Rosangela Dittrich, que abriram as portas do laboratório para as análises.

Ao Laboratório Lumine, às suas colaborados e em especial à Eduarda Sampaio, que proporcionou a realização dos exames de triagem.

Aos colegas e colaboradores da Arca de Noé – Clínica Veterinária, em especial aos enfermeiros Karen Gaspar, Elvis Lisboa, Marlon Cordeiro e William Tacconni, que me ajudaram com limpeza e movimentação de pacientes.

Aos colegas de tatame do jiu-jitsu, cuidar do corpo e da mente foi melhor com vocês.

Toda vez que eu fizer tudo errado é uma chance de praticar.

(Marshall Rosenberg, 2006)

RESUMO

O bloqueio do plano quadrado lombar (QL-Block) é uma técnica de anestesia regional guiada por ultrassom (US) que envolve a infiltração de anestésico local adjacente ao músculo quadrado lombar (QL), proporcionando analgesia abdominal. Foi realizada ampla revisão de literatura englobando a anatomia detalhada da região, a analgesia abdominal e as soluções utilizadas na técnica de bloqueio do plano quadrado lombar. Também foi demonstrada a colocação de cateteres para analgesia contínua no plano interfascial entre o músculo quadrado lombar (QL) e o músculo psoas menor (Pm) sendo aplicada a técnica em três cães com dor abdominal aguda grave devido a peritonite, lobectomia hepática e nefrectomia. Paralelamente, um estudo cadavérico foi conduzido para avaliar a dispersão de solução corante injetada no QL-Block, comparando as abordagens intermuscular (IM) e lateral lombar (LL). Para esta etapa, foram utilizados diferentes volumes de injetado (0.15, 0.3 e 0.6 mL kg^{-1}) em 58 cadáveres, totalizando 116 hemiabdomens caninos para analisar a dispersão craniocaudal e dorsoventral (medidas em centímetros), além da coloração dos ramos ventrais dos feixes nervosos toracolombares (VBSN). O estudo cadavérico analisou a influência de características morfométricas dos cães (peso, comprimento axial, circunferências torácica e abdominal e escore de condição corporal) e de qualidade de obtenção da imagem no US (visualização das estruturas, da agulha e da bolha de injetado). Além disso, o potencial analgésico visceral do QL-Block foi avaliado, considerando sua capacidade de atingir o tronco simpático e contribuir para o controle da dor visceral. Como parte do estudo, propôs-se um modelo matemático para prever o volume necessário de injetado com base nas características morfométricas individuais de cada cão, permitindo a personalização da técnica e potencialmente otimizando a técnica do bloqueio. Quanto ao estudo da passagem dos catéteres, os cateteres foram posicionados bilateralmente e administrou-se bupivacaína intermitente a cada 12 horas, resultando em redução significativa da necessidade de analgesia de resgate e proporcionando um período pós-operatório com menor dor. No estudo cadavérico, os resultados mostraram que a dispersão da solução corante foi semelhante nas abordagens IM ou LL e foi influenciada pelo volume injetado, mas volumes superiores a 0,3 mL kg^{-1} não aumentaram significativamente o número VBSN corados. Porém, IM apresentou maior coloração do tronco simpático, sugerindo um maior potencial para analgesia visceral. O modelo matemático para prever o volume necessário de injetado no plano quadrado lombar (QLP) demonstrou capacidade semelhante ao volume de 0.3 mL kg^{-1}, com variação entre 0.2 e 0.4 mL kg^{-1}. A passagem de catéter no QLP demonstrou ser uma estratégia viável para analgesia prolongada, reduzindo a dependência de opioides e promovendo maior conforto aos pacientes. Não houve influência das abordagens selecionadas para a técnica do QL-Block e o número de VBSN corados, o volume é a variável de maior influência na capacidade de dispersão da técnica, porém com limitações acima de 0.3 mL kg^{-1}. O modelo matemático demonstrou potencial em ser capaz de prever o volume necessário para atingir o limite máximo de benefício do QL-Block em cães.

Palavras-chave: anestesia regional; bloqueios guiados por ultrassom; dor; peritonite.

ABSTRACT

The quadratus lumborum plane (QL-Block) is an ultrasound (US)-guided regional anesthesia technique that involves the infiltration of local anesthetic adjacent to the quadratus lumborum (QL) muscle, providing abdominal analgesia. An extensive literature review was conducted covering the detailed anatomy of the region, abdominal analgesia, and the solutions used in the QL-Block technique. The placement of catheters for continuous analgesia in the interfascial plane between the quadratus lumborum muscle (QL) and the psoas minor muscle (Pm) was also demonstrated, with the technique applied in three dogs with severe acute abdominal pain due to peritonitis, hepatic lobectomy, and nephrectomy. In parallel, a cadaveric study was conducted to evaluate the spread of dye solution injected during QL-Block, comparing intermuscular (IM) and lateral lumbar (LL) approaches. For this stage, different injection volumes (0.15, 0.3, and 0.6 mL kg^{-1}) were used in 58 cadavers, totaling 116 canine hemiabdomens, to analyze craniocaudal and dorsoventral spread (measured in centimeters), as well as the staining of the ventral branches of the thoracolumbar nerve bundles (VBSN). The cadaveric study analyzed the influence of dogs' morphometric characteristics (weight, axial length, thoracic and abdominal circumferences, and body condition score) and the quality of US image acquisition (structure visualization, needle, and injectate bubble). In addition, the visceral analgesic potential of QL-Block was evaluated, considering its ability to reach the sympathetic trunk and contribute to visceral pain control. As part of the study, a mathematical model was proposed to predict the necessary injectate volume based on each dog's individual morphometric characteristics, allowing for technique personalization and potentially optimizing the block. As for the catheter placement study, catheters were placed bilaterally, and intermittent bupivacaine was administered every 12 hours, resulting in a significant reduction in the need for rescue analgesia and providing a postoperative period with less pain. In the cadaveric study, results showed that the spread of the dye solution was similar in both IM and LL approaches and was influenced by the injected volume, but volumes above 0.3 mL kg^{-1} did not significantly increase the number of stained VBSN. However, IM showed greater staining of the sympathetic trunk, suggesting a higher potential for visceral analgesia. The mathematical model to predict the necessary injectate volume in the quadratus lumborum plane (QLP) demonstrated similar effectiveness to the fixed volume of 0.3 mL kg^{-1}, with variation between 0.2 and 0.4 mL kg^{-1}. The catheter placement in the QLP proved to be a viable strategy for prolonged analgesia, reducing opioid dependence and promoting greater patient comfort. There was no influence of the selected approach (IM or LL) on the number of stained VBSN. Volume was the variable with the greatest influence on the spread capacity of the technique, although with limitations above 0.3 mL kg^{-1}. The mathematical model showed potential to predict the necessary volume to reach the maximum benefit threshold of the QL-Block in dogs.

Keywords: pain; peritonitis; regional anesthesia ultrasound-guided blocks.

LIST OF FIGURES

LIST OF TABLES

LIST OF ABBREVIATIONS OR ACRONYMS

IM – Intermuscular Approach

IV - Intravenously

L1 – First Lumbar Vertebra

L2 – Second Lumbar Vertebra

L3 – Third Lumbar Vertebra

L4 – Fourth Lumbar Vertebra

LL – Lateral Lumbar Approach

OIA – Internal Abdominal Oblique Muscle

OEA – External Abdominal Oblique Muscle

PM – Psoas Major Muscle

Pm – Psoas Minor Muscle

QL – Quadratus Lumborum Muscle

QLP – Quadratus Lumborum Plane

TAP – Transversus Abdominis Muscle

T11 – Eleventh Thoracic Vertebra

T12 – Twelfth Thoracic Vertebra

T13 – Thirteenth Thoracic Vertebra

US – Ultrasound

VBSN – Ventral Branches of Spinal Nerves

SUMÁRIO

1 INTRODUCTION

The QL-Block is an ultrasound (US)-guided regional anesthesia technique in which a local anesthetic is infiltrated adjacent to the quadratus lumborum muscle (*m. quadratus lumborum* - QL) with the intention of providing somatic and visceral abdominal analgesia (Elsharkawy et al. 2019). It was first described in dogs for this purpose in 2020 (Garbin et al. 2020a).

The nerve branches that innervate the abdominal wall in dogs emerge from the spinal nerves between the seven, eight or ninth thoracic vertebra and the third lumbar vertebra (Castañeda-Herrera et al. 2017). They begin their course after exiting the central nervous system, subdividing into a ventral branch and a dorsal branch (Evans e Lahunta 2013).

The ventral branches of the spinal nerves (VBSN) are distributed within the quadratus lumborum plane (QLP), located between the QL, psoas minor muscle (*m. psoas minor* - Pm), and psoas major muscle (*m. psoas major* - PM), along the subserosal thoracolumbar fascia (*fascia thoracolumbalis*). These branches traverse the aponeurosis of the transversus abdominis muscle (TAP) and continue toward the ventral midline (Viscasillas et al. 2021a). A branch from each ventral ramus projects medially shortly after exiting the spinal canal, connecting to the sympathetic ganglia, which give rise to the sympathetic trunk (*truncus sympathicus*) (Evans e De Lahunta 2013).

The local anesthetic injected into the QLP spreads through the thoracolumbar fascia, where the VBSN of the thoracolumbar nerves responsible for abdominal wall innervation are located (Garbin et al. 2020), with the potential to provide visceral analgesia due to possible spread over the sympathetic trunk (Viscasillas et al. 2021a).

1.1 PROBLEM

Considering the use of QL-Block as part of an analgesic protocol for managing abdominal pain in dogs appears promising. However, this technique involves multiple variables, including potential variations in the final positioning of the needle tip, patient-specific anatomical differences, the resolution and capabilities of the US equipment used, and the operator’s level of expertise. These factors contribute to uncertainties regarding the most effective and standardized approach to performing this technique in dogs.

1.2 Objectives

1.2.1 General objective

To enhance and refine the knowledge on the efficacy and clinical applicability of QL-Block as an abdominal analgesia technique in dogs, considering different US-guided approaches, injection volumes, morphometric characteristics, and their impact on the block's spread and effectiveness.

1.2.2 Specific Objectives

- **Propose the use of intermittent analgesia catheters:** To report the applicability and effectiveness of catheter placement in the QLP for continuous analgesia in cases of severe abdominal pain.
- **Evaluate injectate spread in the QLP:** To compare the intermuscular (IM) and lateral lumbar (LL) approaches in terms of craniocaudal and dorsoventral spread of the dye solution, as well as the staining of thoracolumbar nerve bundles.
- **Investigate anatomical and technical factors:** To determine to what extent morphometric characteristics (weight, spinal length, thoracic circumference, abdominal circumference, and body condition score) and US image quality scores (ultrasonographic imaging, needle visualization, and injectate volume visualization) affect the spread outcomes in QL-Block.
- **Predict the contribution on visceral analgesia:** To evaluate the capacity of different QL-Block approaches to reach the sympathetic trunk and, consequently, infer their contribution to visceral analgesia.
- **Explore Technical Limitations:** To identify challenges related to needle positioning, US visualization, and block execution in dogs of varying body sizes and conditions.
- **Present Practical Recommendations:** To propose effective methods for performing QL-Block in dogs, including injectate volumes and technical approach.
- **Individualize Injectate Volume:** To propose an equation for performing the QL-Block technique in dogs and validate its use both intra and inter- operator**.**

1.3 RATIONALE

QL-Block is a promising US-guided regional anesthesia technique for abdominal analgesia in dogs. The described anatomy of the thoracolumbar interfascial region suggests that QL-Block may be advantageous due to its potential for injectate

spread over the thoracolumbar nerve bundles responsible for abdominal wall innervation, with the added proximity to the sympathetic trunk. However, there is still no consensus on the most effective technique to ensure adequate injected spred over these nerve bundles.

Therefore, understanding the variables that influence the spread capacity of QL-Block and exploring more consistent alternatives to prolong its anesthetic effect is essential for optimizing the use of this technique in veterinary medicine, contributing to advancements in analgesia and animal welfare.

2 LITERATURE REVIEW

The region where injectate spread occurs in the QL-Block technique can be referred to as the thoracolumbar hypaxial region. This area consists of important bones, muscular, fascial, vascular, and neural structures (Figure 1).

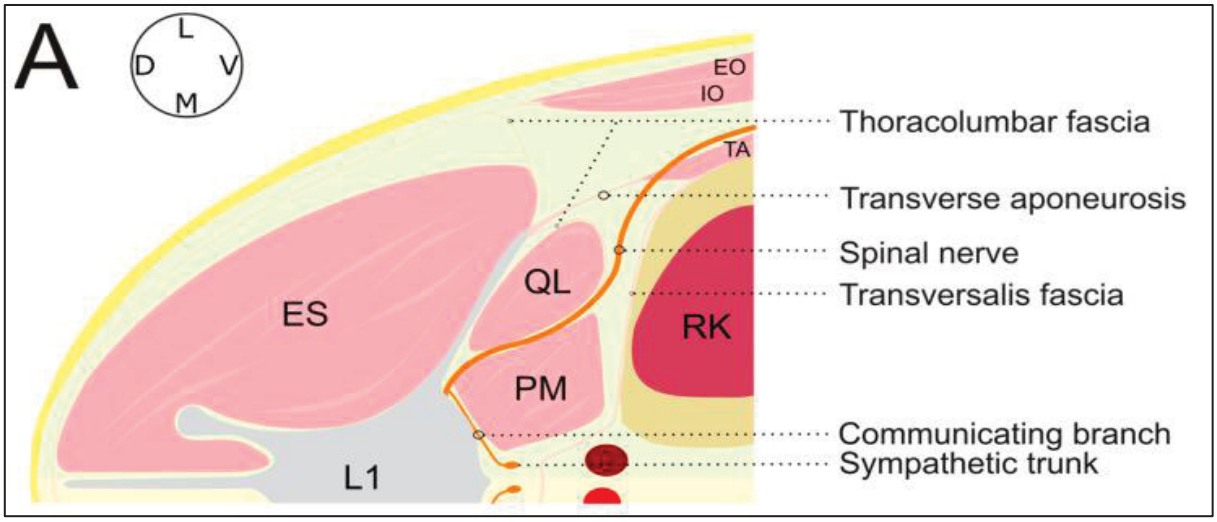

Figure 1. (A) Schematic illustration of the craniocaudal view anatomy at the level of the first lumbar vertebra in a dog positioned in lateral recumbency (Marchina-Gonçalves et al. 2023).

* QL - Quadratus lumborum muscle; PM - Psoas minor muscle; EO - External abdominal oblique muscle; IO Internal abdominal oblique muscle; TA - Transversus abdominis muscle; ES - Erector spinae muscle group; L1 - First lumbar vertebra; RK – Right kidney.

2.1 ANATOMY

2.1.1 Bones

Since it is performed at the level of the first lumbar vertebra (L1), the QL-Block may result in injectate spread from the last thoracic vertebrae or through the cranial portion of the lumbar vertebrae (Garbin et al. 2020a, Alaman et al. 2022).

There are 13 thoracic vertebrae, which have shorter vertebral bodies compared to the lumbar vertebrae. The first nine thoracic vertebrae are similar, featuring long spinous processes that incline caudally, while the last four (T10–T13) exhibit structural variations. The eleventh thoracic vertebra (*vertebra anticlinalis* - T11) is known as the anticlinal vertebra because its spinous process is nearly perpendicular to the bony axis, marking the thoracolumbar transition. From the twelfth thoracic vertebra (T12) onward, the spinous processes incline cranially. Additionally, the last three thoracic vertebrae each have only a single complete costal fovea per side (Hermanson et al. 2020a).

There are seven lumbar vertebrae. They have longer and wider bodies

compared to the thoracic vertebrae, progressively increasing in size up to the fifth lumbar vertebra (Lacowicz et al., 2024). The transverse processes are directed cranially and ventrally. The thoracolumbar region typically consists of 20 vertebrae, with cases of 21 vertebrae being extremely rare (Hermanson et al. 2020a).

2.1.2 Muscles

The QL muscle is enveloped by the thoracolumbar fascia group, ventrally positioned in direct contact with the bodies of all lumbar vertebrae and the last three thoracic vertebrae, precisely lateralized ventral to the transverse processes of the lumbar vertebrae and the proximal region of the last two ribs. Its insertion occurs on the medial surface of the ilium wing, between the articular surface and the cranial ventral iliac spine (Hermanson 2020).

Adjacent to the QL and enveloped by the thoracolumbar fascia are the *psoas minor* muscle (Pm) and the *psoas major* muscle (PM). The Pm, visible caudal to L1, is located dorsally to the peritoneum and ventrally to the QL. In the most caudal portion, the PM, visible caudal to the fourth lumbar vertebra (L4), is positioned ventrally to the QL and dorsally to the *Pm* (Hermanson 2020, Viscasillas et al. 2021a).

2.1.3 Fasciae

The fasciae of the trunk are divided into superficial and deep layers. They are composed of dense connective tissue that covers the muscles and bones of the thorax and abdomen. The internal trunk fascia (*fascia interna trunci*) lines the deep surface of the body wall muscles and the outer surface of the serous linings of the body cavities. It is referred to as the endothoracic fascia (fascia endothoracica) in the thorax and the transversalis fascia (fascia transversalis) in the abdomen (Hermanson 2020).

The thoracolumbar fascia is a dense, tendinous membrane that provides structural support to the dorsal region. It originates from the spinous processes of the thoracic and lumbar vertebrae and the supraspinous ligament. Its structure consists of two layers. The superficial layer gives rise to the muscles latissimus dorsi (*latissimus dorsi*), abdominal oblique (*obliquus externus abdominis; obliquus internus abdominis*), and caudal dorsal serratus (*serratus dorsalis caudalis*). The deep layer provides insertion for the splenius (*splenius*), cranial dorsal serratus (*serratus dorsalis cranialis*), muscle retractor costae and TAP (Hermanson 2020).

2.1.4 Arteries

The abdominal aorta (*aorta abdominalis*) is one of the most ventral structures in the hypaxial region. It terminates near the seventh lumbar vertebra (L7), bifurcating into the right and left internal iliac arteries (*aa. iliacae internae dextra et sinistra*) and the median sacral artery (*a. sacralis mediana*). Along its course, it is slightly deviated to the left by the caudal vena cava (*v. cava caudalis*) and is positioned within a groove formed between the right and left PM (Hermanson et al. 2020b).

Near the vertebral body of L1, the cranial abdominal arteries (aa. abdominalis cranialis) may arise from the lateral portion of the abdominal aorta, originating from the phrenicoabdominal trunk. These blood vessels run parallel to the ribs, piercing the ventral surface of the Pm/PM group, and function to supply the cranial abdominal wall (Hermanson et al. 2020b).

2.1.5 Veins

The caudal vena cava is formed by the convergence of the common iliac veins (*vv. iliacae communes*) near L7. It is located alongside the abdominal aorta, within the groove formed by the bilateral PM. Near L1, its course is projected toward the right side of the abdomen (Hermanson et al. 2020c).

The phrenicoabdominal trunk also consists of veins, considered satellite and homonymous tributaries of the arteries they accompany (i.e., cranial abdominal veins). These veins drain blood from the cranial abdominal wall and its adjacent muscles (Hermanson et al. 2020c).

2.1.6 Nerve Branches

The somatic innervation of the abdominal wall originates primarily from the ventral branches of the spinal nerves (VBSN) of the ninth thoracic spinal nerve and extends to the VBSN of the third lumbar spinal nerve (Hermanson et al. 2020d). However, anatomical variations may occur between individuals, and the VBSN of the seventh and eighth thoracic spinal nerves may also contribute (Castañeda-Herrera et al. 2017). When QL-Block is performed, the injectate spreads to at least the first three lumbar segment VBSN, but it may also reach the last thoracic nerves (Garbin et al. 2020a; Viscasillas et al. 2021; Marchina-Gonçalves et al. 2023).

The thoracic spinal nerves give rise to a dorsal branch and a ventral branch. The VBSN are commonly referred to as intercostal nerves. In the caudal portion of the

thorax, near the vertebral body, muscular layers of the internal intercostal muscle cover the nerves. The intercostal nerve bundles from T11 and T12 only emit long lateral cutaneous branches, which innervate the ventral midline. The last thoracic nerve, known as the costoabdominal nerve (*n. costoabdominalis*), innervates the abdominal wall adjacent to the caudal edge of the last rib and runs tangentially along the costal arch until it reaches the ventral midline, where, similarly to the lumbar nerves, it subdivides into a lateral (*cutaneous*) branch and a medial branch (Hermanson et al. 2020d).

Named L1 (cranial iliohypogastric nerve / *n. iliohypogastricus cranialis*), L2 (caudal iliohypogastric nerve / *n. iliohypogastricus caudalis*), and L3 (ilioinguinal nerve / *n. ilioinguinalis*), they are responsible for the innervation of the abdominal wall caudal to the umbilical scar (Hermanson et al. 2020d).

The cranial and caudal iliohypogastric nerves give off medial branches (muscular branches to the QL, Pm, and PM). They pierce the QL segments and run along the endothoracic fascia, penetrating the fascia that separates the TAP from the internal abdominal oblique (OIA) (Hermanson et al. 2020d).

The cranial iliohypogastric nerve branches into lateral and medial subdivisions after leaving the thoracolumbar fascia. The lateral subdivision runs between the OIA and external abdominal oblique (OEA), extending toward the midline, where it gives off a cutaneous branch. The medial subdivision continues between the OIA and TAP, providing innervation to the peritoneum and musculature, similarly to the last five thoracic nerves (Hermanson et al. 2020d). These branches are targeted in the transversus abdominis plane block (TAP-Block) (Freitag et al. 2020).

The caudal iliohypogastric nerve follows a path similar to that of the first lumbar nerve, except that it innervates the abdominal wall caudal to it and emerges at the lateral border of the hypaxial musculature after passing between the quadratus lumborum and the iliopsoas muscles at the lumbocostal arch. Its lateral subdivision does not give off a cutaneous branch, and in some cases, the ventral branch may be duplicated, leading to a reduction in the third lumbar nerve, and rarely is a single nerve formed by the fusion of the first and second or the second and third lumbar nerves. (Hermanson et al. 2020d).

The ilioinguinal nerve gives off medial branches that innervate the PM and may anastomose with the fourth lumbar nerve. It divides into a lateral branch, responsible for innervating the skin on the craniolateral surface of the thigh, and a ventral branch,

which is small and projects caudally. Occasionally, one of the iliohypogastric nerves may be duplicated, with a reciprocal reduction in the size of the nerve located caudal to it. Rarely, the first and second or the second and third lumbar nerves may fuse to form a single nerve (Hermanson et al. 2020d).

Within the subserosal endothoracic fascia, the lumbar plexus (*plexus lumbalis*) is also found. This plexus provides innervation to the cranial and medial thigh muscles and the skin on the medial surface of the pelvic limb. It is formed by the VBSN of the third, fourth, and fifth lumbar nerves, which are interconnected (Hermanson et al. 2020d).

Some important nerve structures could be at least partially blocked by performing the QL-Block at the level of L1 (Garbin et al. 2020a; Marchina-Gonçalves et al. 2023). These include the genitofemoral nerve (*n. genitofemoralis*), the lateral cutaneous femoral nerve (*n. cutaneus femoris lateralis*), and the femoral nerve (*n. femoralis*) (Hermanson et al. 2020d).

The genitofemoral nerve innervates the proximal skin of the medial thigh and the genital branches of the pudendal region. It is formed by the union of the VBSN of the third and fourth lumbar nerves, although it may receive contributions from the second lumbar nerve and sometimes lacks contribution from the fourth lumbar nerve. It is located in the medial portion of the PM, near the body of L4, and courses caudally, running close to the caudal vena cava and abdominal aorta. It then emerges through the inguinal canal, where it innervates the previously mentioned structures (Hermanson et al. 2020d).

The lateral cutaneous femoral nerve is primarily formed by the projection of the fourth lumbar nerve, although it is very common for it to have connections with the third lumbar nerve and, more rarely, with the fifth lumbar nerve. Its course runs caudolateral to the Pm, giving off branches to hypaxial structures and being responsible for a large portion of the cutaneous innervation of the craniolateral thigh (Hermanson et al. 2020d).

The femoral nerve originates from the fifth lumbar nerve and has important connections with the fourth and sixth lumbar nerves. It arises from the caudal portion of the PM and follows a caudal trajectory until it exits the abdomen, traveling alongside the iliopsoas muscle (Hermanson et al. 2020d).

The sympathetic trunk extends continuously along the thoracic and lumbar vertebrae. The nerve bundle responsible for the sympathetic innervation of the cranial

abdominal viscera is the greater splanchnic nerve (n. splanchnicus major), which joins the celiacomesenteric plexus and originates from the thirteenth thoracic ganglion (Evans and De Lahunta 2013), passing dorsally to the lumbocostal arch to enter the abdominal cavity. These nerves innervate structures such as the spleen, liver, stomach, small intestine, large intestine, and pancreas (Hermanson et al. 2020d).

The lumbar portion of the sympathetic trunk originates from all spinal segments. The first lumbar nerve contributes to the innervation of the cranial abdominal viscera through its connection with the celiacomesenteric plexus, which penetrate the abdominal cavity between the lumbocostal arch and the psoas musculature. The more caudal lumbar nerves participate in the formation of ganglia responsible for the innervation of major blood vessels, kidneys, urinary bladder wall, small intestine, large intestine, and gonads (Hermanson et al. 2020d).

2.2 ABDOMINAL ANALGESIA

Pain is triggered by intense, potentially harmful stimuli, leading to the release of inflammatory mediators (algogenic substances) such as bradykinin, serotonin, histamine, potassium ions, acetylcholine, interleukin-1, nitric oxide, and proteolytic enzymes. Additionally, prostaglandins and substance P enhance the sensitivity of nerve endings, although they do not directly excite them (Afridi et al. 2021, Andrade et al. 2008).

Sensory fibers are classified into Aβ, Aδ, and C, based on diameter, degree of myelination, and conduction velocity, in decreasing order (Garcia, 2017). Pain-specific receptors are located at the nerve endings of Aδ and C fibers, with C fibers having a slower conduction velocity than Aδ fibers (Grundy et al. 2019).

Viscera contain pain specific sensory receptors (Andrade et al., 2008), which are predominantly mediated by C fibers (Grundy et al., 2019). As a result, localized visceral damage rarely causes severe pain, whereas any diffuse stimulation of these nerve endings induces intense pain (Hall e Guyton, 2011).

Parietal surfaces, in turn, have somatic innervation. As a result, mechanical stimuli, such as incisions, can be extremely painful. Additionally, chemical agents, including inflammatory mediators and bacteria, can activate nociceptors in the parietal portion of the peritoneum, intensifying the pain sensation (Hall e Guyton, 2011).

Pain conduction to the brain occurs through two ascending pathways. The neospinothalamic tract, responsible for somatic pain transmission and

paleospinothalamic tract, responsible for visceral pain transmission (Andrade et al., 2008). The paleospinothalamic pathway is further subdivided into True visceral pain pathway (conducts impulses via the sympathetic trunk, leading to pain sensations perceived in body surfaces distant from the affected organ) and parietal pathway (conducts pain directly through the VBSN of spinal nerves, resulting in well-localized pain perception (Hall e Guyton, 2011).

2.2.1 Peritonitis

Peritonitis is associated with a high mortality rate in dogs (Barfield et al. 2015). It frequently occurs in critically ill patients requiring intensive care, often presenting with severe pain and paralytic ileus (Spackman e Cullen 2000), pancreatitis episodes (Freitag et al. 2018), or gastrointestinal tract surgeries (Barfield et al. 2015).

In dogs, few case reports describe the clinical applicability of QL-Block, with limitations regarding analgesic effectiveness (Watanabe et al. 2024), or the placement of a catheter in the QLP (Camargo-Fontanela et al. 2024; Degani et al. 2024) in patients with peritonitis. Additionally, it has been reported that sympathetic ganglion blockade should be approached with caution in severe septic peritonitis caused by Gram-negative bacteria that fail to respond adequately to antimicrobial treatment (Solomon et al. 2003).

2.2.2 Spaying Surgery

The innervation of the ovary is provided by the sympathetic trunk ganglia from the VBSN of the tenth thoracic to the sixth lumbar segments, with the highest concentration between T13 and L3 (Hermanson et al. 2020d). The structure that anchors the ovary to the abdominal wall is called the mesovarium, a double peritoneal fold, whose root is directly innervated by somatic nerve bundles from L2 and L3 (König e Liebich 2012, Budras et al. 2012).

In female dogs, two clinical trials have evaluated the efficacy of QL-Block for spaying. One study assessed its use for ovariohysterectomy (OH) with 0.25% bupivacaine at an injectate volume of 0.4 mL kg^{-1} (Viscasillas et al. 2021b), while another investigated its application in ovariectomy (OE) using 0.33% or 0.5% ropivacaine at an injectate volume of 0.3 mL kg^{-1} (Degani et al. 2023). Both studies demonstrated postoperative pain control benefits with QL-Block.

2.2.3 Meta-Analyses

Clinical applicability studies of QL-Block are more advanced in humans. Over the past five years, 34 meta-analyses have been published, reviewing its use in abdominal surgeries. The results indicate a benefit from QL-Block application. However, only six of these meta-analyses have a high level of evidence, demonstrating the superiority of QL-Block compared to TAP-Block (Liu et al. 2020, Barry et al. 2023, Wang et al. 2020, Gao et al. 2024) or the continuous infusion of opioids (Xu et al. 2020). This superiority is attributed to better postoperative pain control, reduced opioid consumption, and lower incidence of vomiting (Zhang et al. 2022).

2.3 SOLUTIONS

For the QL-Block technique, the choice of solution to be injected into the thoracolumbar fascia must be considered. Dye solutions (Alaman et al. 2022) and iodinated contrast agents (Degani et al. 2024) are commonly used in cadaveric studies, while local anesthetic solutions are used *in vivo* (Degani et al. 2023). A combination of these solutions may also be used at the researcher's discretion to simulate *in vivo* spread (Garbin et al. 2020a) or to ensure advanced imaging acquisition (Viscasillas et al. 2021). However, studies suggest that containing iodinated contrast solutions may reduce spread capacity (Miguel-Garcia et al. 2020).

2.3.1 Dyes

Dye is used to observe the spread of the solution over the VBSN of the thoracolumbar nerve bundles during QLP dissection in cadavers. The most commonly used dye is methylene blue (Viscasillas et al. 2021a, Alaman et al. 2022, Marchina-Gonçalves et al. 2022, Marchina-Gonçalves et al. 2023), followed by tissue-specific permanent marking dyes (Garbin et al. 2020a, Garbin et al. 2020b).

2.3.2 Contrast

Contrast is used for advanced imaging acquisition and for assessing the spread of the solution in the QLP, by counting the number of vertebrae without the influence of dissection manipulation or when dissection is not feasible. Iodinated contrast and computed tomography are the reported methods for imaging, both *post-mortem* (Viscasillas et al. 2021a, Marchina-Gonçalves et al. 2022, Marchina-Gonçalves et al. 2023) and *in vivo* (Viscasillas et al. 2021b, Degani et al. 2024).

2.3.3 Local Anesthetics

Local anesthetics can be used to mimic the in vivo spread of dye in cadaveric studies, with lidocaine being reported (Garbin et al. 2020a, Garbin et al. 2020b). In clinical trials, long-acting anesthetics are used to evaluate the abdominal pain relief that QL-Block can provide in dogs (Viscasillas et al. 2021b, Degani et al. 2023, Camargo-Fontanela et al. 2024, Degani et al. 2024).

2.3.3.1 Bupivacaine

Strongly lipophilic, four times more potent than lidocaine, with an onset of action between 20 and 30 minutes and a duration of up to 10 hours (Garcia7 2017). Its use has been reported as an adjunct for pain management caused by peritonitis in dogs, administered every 12 hours (Camargo-Fontanela et al. 2024), and its clinical applicability for OSH surgery has been demonstrated, showing a reduction in the need for rescue analgesia (Viscasillas et al. 2021b).

2.3.3.2 Ropivacaine

Marketed in its pure S-enantiomer form to reduce toxicity, it is less potent than bupivacaine, with a block duration of up to six hours. However, it exhibits a biphasic effect on peripheral vascularization, potentially causing vasoconstriction as well (Garcia 2017). Its use has been reported with QLP catheter placement for abdominal surgeries with high pain potential, administered every 8 hours (Degani et al. 2024). Additionally, its clinical applicability for OE surgery has been demonstrated, showing postoperative pain control in QL-Block groups and a significant increase in time to first rescue at higher concentrations (Degani et al. 2023).

* Anatomical variations found during the dissection of the dogs in this study are described in Supplementary Material 1.

3 - PRELIMINARY EXPERIENCE WITH QUADRATUS LUMBORUM CATHETERS FOR INTERMITTENT ANALGESIA IN THREE DOGS WITH ACUTE ABDOMINAL PAIN

Marco Aurélio Camargo Fontanela[a] ; Paulo Roberto Klaumann[b]; Robson Junior Piontkovski[c] ; Priscila Souza Ferreira[c]; Fabiano Montiani-Ferreira[a] ; Juan Carlos Duque Moreno[a]

a - Department of Veterinary Medicine, Federal University of Parana, Curitiba, PR, Brazil
b - Veterinary Anesthesia Service, Curitiba, PR, Brazil
c - Veterinary Teaching Hospital, Federal University of Parana, Curitiba, PR, Brazil

MACF: study design, acquisition of data, analysis and interpretation of data, preparation of manuscript.
PRK and FM: analysis and interpretation of data, critical revision of manuscript.
RJP and PSF: acquisition of data, analysis and interpretation of data.
JCDM: study design, acquisition of data, analysis and interpretation of data, preparation and critical revision of manuscript.

DOI: https://doi.org/10.1016/j.vaa.2024.05.010

The QL-block, an US-guided regional anesthesia technique, entails injecting local anesthetic into the interfascial space enclosing the QL (Garbin et al. 2020). It has been used successfully for ovari-ectomy and ovariohysterectomy surgeries in dogs (Viscasillas et al. 2021; Degani et al. 2023). Additionally, interfascial catheter implantation has been described to facilitate locoregional techniques, such as the TAP-Block in dogs (Freitag et al. 2018) and the QL-block in human pediatric patients (Pooley et al. 2022). This report describes bilateral catheter implantation into the interfascial plane between the QL and Pm at the level of the first lumbar vertebra for multimodal analgesia in three dogs admitted to an intensive care unit. Dog 1 was a 12 year old Shih Tzu [7.5 kg, body condition score 4/9] experiencing moderate to severe pain attributed to peritonitis. The dog was not responding adequately to methadone [0.3 mg kg^{-1} intramuscularly, (Mytedom, 10 mg mL^{-1} , Cristalia, Brasil)] and dipyrone [25 mg kg^{-1} subcutaneously (SC), D-500, 500 mg mL^{-1} , Zoetis, Brasil], with a score of 10/24 on the Glasgow Composite Measure Pain Scale-Short Form [CMPS-SF] (Reid et al. 2007). Dog 2 was an 11 year old, mixed breed female dog (10.2 kg, body condition score 6/9), which had undergone hepatic lobectomy. Tenderness of the abdominal wall was noted on palpation, with a CMPS-SF pain score of 13/24 postoperatively. Two

continuous infusions were delivered intravenously (IV), resulting in sedation but not analgesia: fentanyl (10 mg kg^{-1} $hour^{-1}$, Fentanest, 0.05 mg mL^{-1} , Cristalia, Brasil), and a separate infusion of lidocaine (2 mg kge1 houre1 , Xylestesin, 20 mg mLe1 , Cristalia, Brasil) and ketamine (1.2 mg kg^{-1} $hour^{-1}$, Ketamina, 100 mg mL^{-1} , Agener União, Brasil). Dog 3 was a 12 year old female French Bulldog (9.3 kg, body condition score 5/9), which underwent nephrectomy.

For catheter implantation, dogs 1 and 2 were anesthetized with repeated IV boluses of propofol and oxygen supplementation was provided by facemask. In dog 3, catheters were implanted after induction of anesthesia, before beginning surgery. Once anesthetized, dogs were positioned in lateral recumbency, overlying fur clipped and the skin aseptically prepared. An 8e15 Hz linear transducer (GE logic f6, L6-12-RS; GE Healthcare, USA) was placed caudal and parallel to the last rib, with the marker facing dorsally. After scanning the thoracolumbar region, as previously described (Garbin et al. 2020), the transverse process of L1 and the erector spinae, QL and Pm muscles were located. The transducer was then rotated approximately 30 degrees in a caudodorsal direction (Fig. 2a) while maintaining an US window (Fig. 2b) similar to that described by Garbin et al. (2020). A 9 cm, 18 gauge Tuohy needle (BD Perisafe; Becton Dickinson, Brasil), connected to an IV extension set filled with 0.5% bupivacaine (Neocaina, 5 mg mLe1 , Cristalia, Brasil), was introduced inplane from caudolateral to craniomedial. The needle tip was directed in the fascial plane between the QL and Pm (Fig. 2c). After confirming correct positioning of the needle by visualizing injection of 0.1 mL of the local anesthetic solution, 0.3 mL kg^{-1} of local anesthetic was injected (Fig. 2d). The IV extension set was disconnected and a 20 gauge catheter (Portex Epidural Catheter, Smiths Medical, Czech Republic) was inserted and advanced approximately 3 cm through the needle (Fig. 2e). After removing the needle, a further 0.5 mL of bupivacaine solution was injected to confirm injectate dispersal into the fascial plane. The catheter was attached to the skin with four simple interrupted nylon sutures and protected with semiocclusive dressing. After completing the first catheter implantation, the dog was repositioned and the procedure was repeated on the contralateral side.

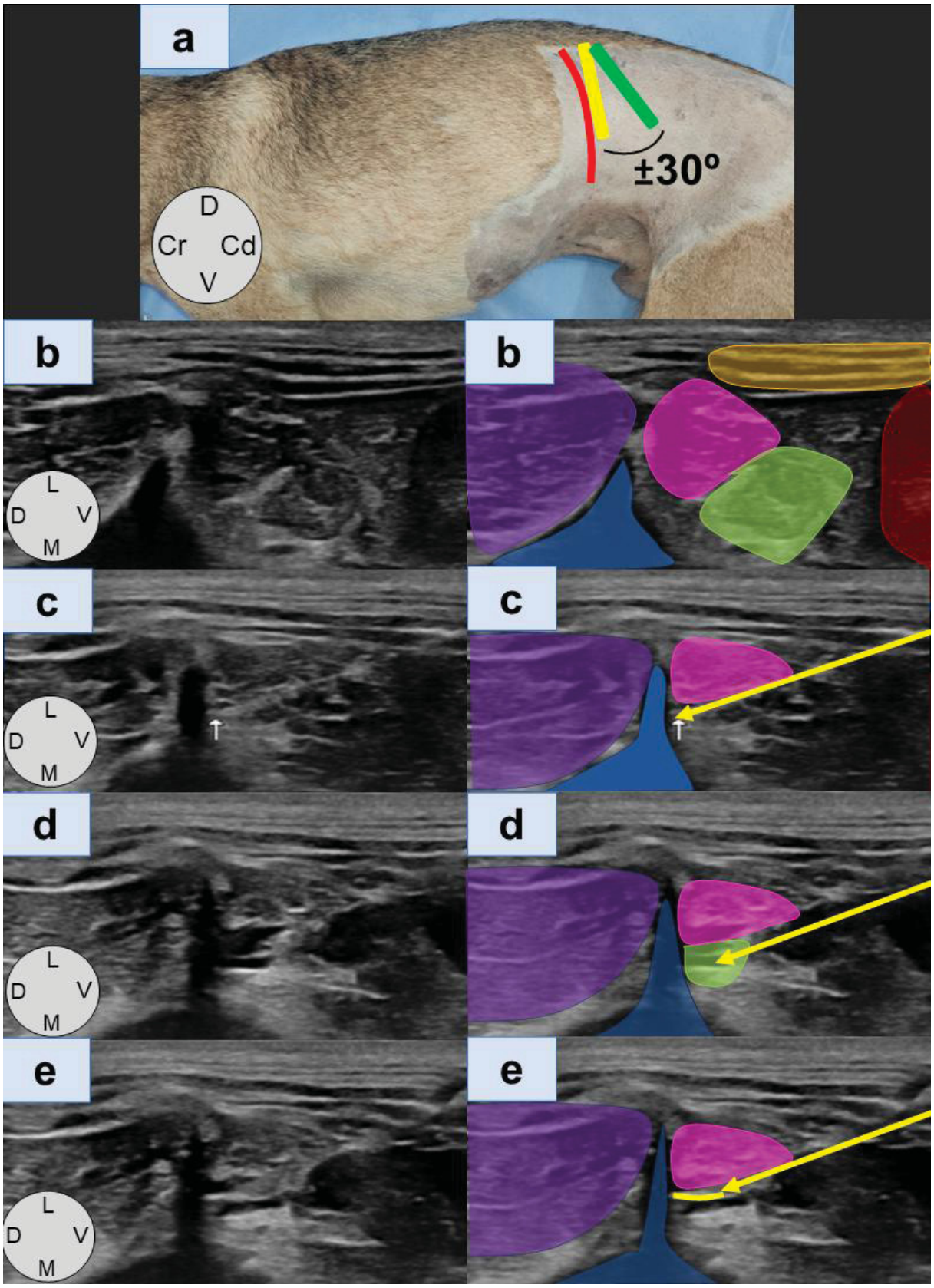

Figure 2. (a) Rotation of the ultrasound transducer by approximately 30 degrees to perform intermittent analgesia after a catheter placement in the interfascial plane between the quadratus lumborum (QL) and psoas minor (PM) muscles demonstrated in a normal dog cadaver. Red line indicates outline of the last rib position, yellow rectangle shows the site for transducer placement, similar to Garbin et al. (2020), green rectangle shows the suggested positioning of the transducer for placing a continuous analgesia catheter. (b) Left side: hypaxial lumbar sonoanatomy images after caudodorsal transducer rotation (all

on the left side). Right side: sonogram highlighting the kidney (in red), abdominal wall muscles (in orange), erector spinae muscle (in purple), QL (in pink), PM (in green) and vertebral transverse process (in blue). (c) Schematic positioning of the needle (yellow arrow) adjacent to the QL (in pink) in the same sonogram. (d) Schematic representation of the moment of local anesthetic injection in the interfascial plane between the QL and PM muscles (in green). (e) Schematic representation of the passage of the epidural catheter (yellow line) in the interfascial plane.

For intermittent analgesia, 0.3 mL kg^{-1} of 0.5% bupivacaine was injected into the catheters bilaterally every 12 hours. If pain scores 6/24 were recorded between injections, rescue analgesia was provided with methadone (0.3 mg kg^{-1} intramuscularly). Pain scores were recorded immediately before catheter insertion and hourly for a period of 12 hours, after which dogs were assessed every 6 hours for at least 72 hours after catheter insertion. Following catheter implantation and injection of bupivacaine in dog 1, dipyrone and methadone were stopped. In dog 2, analgesic infusions were stopped and the dog was administered only two methadone rescue doses, 10 and 36 hours after catheter insertion (CMPS-SF score 6/24), close to the scheduled bupivacaine injections. In dog 3, an opioid-free postoperative period was possible for 7 days. The authors assert that approaches involving positioning the probe parallel to the rib and directing the needle towards the vertebral body make it more challenging to advance the catheter cranially into the interfascial plane. Likewise, if the probe is oriented perpendicular to the rib, achieving proper positioning of the needle tip in the appropriate plane will be more challenging (Garbin et al. 2020a). Computed tomography would confirm catheter positioning better, but logistical and financial constraints prevented its use. Consequently, catheter migration, while still providing analgesia, cannot be ruled out. While this report is limited to three cases, the results indicate that injection of 0.5% bupivacaine through catheters implanted in the interfascial plane between the QL and Pm could be a useful contribution to multimodal analgesia for effectively managing abdominal pain resulting from abdominal surgery or peritonitis. Analgesia achieved in these dogs, which had pain originating from the cranial abdomen, does not align with dye and contrast medium dispersion observed in cadaveric studies. However, as noted by Viscasillas et al. (2021b), the spread of local anesthetic may exceed that of contrast agents. It is also possible that there is diffusion of local anesthetic into other layers of tissue and analgesia from a systemic effect secondary to absorption and redistribution (Chin et al. 2021).

*Images of cadaver dissection, contrast-enhanced radiography, and magnetic resonance imaging after catheter passage in the QLP of dogs are found in Supplementary Material 2.

4 - INFLUENCE OF MORPHOMETRIC CHARACTERISTICS AND VOLUME ON DYE SOLUTION SPREAD IN THE QUADRATUS LUMBORUM PLANE VIA INTERMUSCULAR OR LATERAL LUMBAR APPROACHES IN CANINE CADAVERS

Marco Aurélio Camargo Fontanela[a]; Marina Moresco[b]; Gilberto Serighelli Júnior[c]; Marcello Machado[d]; Fabiano Montiani-Ferreira[e]; Juan Carlos Duque Moreno[F]

a - Veterinary Sciences Graduate Program, Department of Veterinary Medicine, Federal University of Paraná, Curitiba – PR, Brazil. ORCID: 0000-0002-9561-5328
b - M.Sc., Self-employed veterinarian, Curitiba, State of Paraná, Brazil ORCID: 0009- 0008-4458-2678
c - Veterinary Sciences Graduate Program, Department of Veterinary Medicine, Federal University of Paraná, Curitiba – PR, Brazil. ORCID: 0000-0002-0979-7939
d - Department of Anatomy, Federal University of Paraná - UFPR, Curitiba – PR, Brazil. ORCID: 0000-0002-8932-6247
e - Department of Veterinary Medicine, Federal University of Paraná - UFPR, Curitiba – PR, Brazil. ORCID: 0000-0002-3933-8864
f* - Department of Veterinary Medicine, Federal University of Paraná - UFPR, Curitiba – PR, Brazil. ORCID: 0000-0003-4048-1198

MACF: study design, acquisition of data, analysis and interpretation of data, preparation of manuscript.
MMb: acquisition of data, analysis and interpretation of data.
GSJ: analysis and interpretation of data, preparation of manuscript.
MMd: analysis and interpretation of data, critical revision of manuscript.
FMF: analysis and interpretation of data, preparation and critical revision of manuscript.
JCDM: study design, acquisition of data, analysis and interpretation of data, preparation and critical revision of manuscript.

*Article under submission in Veterinary Anasthesia and Analgesia.

ABSTRACT

Objective: To compare dye spread following injection in the quadratus lumborum plane (QLP) via intermuscular (IM) and lateral lumbar (LL) approaches with different volumes in canine cadavers of different sizes.

Study Design: Cadaveric, experimental, and prospective study.

Animals: Fifty-eight canine cadavers.

Material and Methods: Morphometric data (weight, body score, axial length, abdominal and thoracic circumference) were collected. Then, US-guided injections of 0.1% methylene blue were performed via IM and LL approaches at volumes of 0.15, 0.3, and 0.6 mL kg^{-1} in the QLP. Animals were classified by body mass as <10 kg (small - S), 10-20 kg (medium - M), or >20 kg (large - L), with procedures performed on both hemiabdomens, totaling 116 injections. Hemiabdomens were dissected to assess dye spread in the craniocaudal and ventrodorsal directions, the number of thoracolumbar ventral branches of spinal nerves (VBSN) stained, and spread to the sympathetic trunk. Technique and dissection times were recorded, along with scores for visibility of sonoanatomic reference structures, needle, and injected solution in the QLP.

Results: Volume was the variable that most influenced spread capacity ($p < 0.0015$). Additionally, craniocaudal spread did not differ significantly between IM and LL and was significantly and directly related to the volume used. However, an increase in the spread did not enhance the number of stained VBSN. The most frequently stained VBSN were L2, L3, and L1. Using 0.6 mL kg^{-1} did not increase the number of stained VBSN. In the IM group, the morphometric variables showed a weaker correlation with the ability to stain the VBSN.

Conclusion and clinical relevance: There was no significant differences in spread between IM and LL. Volume affects spread, but amounts over 0.3 mL kg^{-1} do not increase the number of stained VBSN. Morphometric variables do not affect the number of stained VBSN.

Keywords: dogs, dye spread, regional anesthesia, sonoanatomy, ultrasound-guided blocks.

4.1 INTRODUCTION

In dogs, five approaches for the QL-Block have been described, allowing ventrodorsal needle positioning (Garbin et al. 2020a; Garbin et al. 2020b; Alaman et al. 2022; Marchina-Gonçalves et al. 2022; Marchina-Gonçalves et al. 2023), along with one distinct and effective dorsoventral positioning option in the intermuscular (IM) plane (Viscasillas et al. 2021a) (Figure 11 – in the Supplementary Material 4).

Despite these varied approaches, the injected solution seems to spread mainly within three planes. The LL when positioned between the lateral surface of the QL, the internal face of the TAP and the ventral thoracolumbar fascia (Garbin et al. 2020b; Marchina-Gonçalves et al. 2023); the IM plane when positioned between the medial surface of the QL muscle and the lateral surface of the Pm muscle (Garbin et al. 2020a; Viscasillas et al. 2021a); and the dorsal plane when positioned between the dorsal surface of the QL/Pm and the transverse process or body of the first lumbar vertebra (Alaman et al. 2022).

There are reports of the use of different volumes of dye solution for injection into the QLP in cadaveric studies. With volumes of 0.15 mL kg^{-1} (Garbin et al. 2020a) and 0.2 mL kg^{-1} (Viscasillas et al. 2021a) the nerve bundles responsible for the sensitivity of the caudal abdominal wall were effectively stained. However, higher volumes, such as 0.3 mL kg^{-1} (Garbin et al. 2020a), 0.5 mL kg^{-1} (Alaman et al. 2022), and 0.6 mL kg^{-1} (Marchina-Gonçalves et al. 2022; Degani et al. 2024), have demonstrated the ability to stain a greater number of nerve bundles (Garbin et al., 2020a; Alaman et al. 2022; Marchina-Gonçalves et al. 2022) or to achieve adjacent spread across a greater number of vertebrae (Degani et al. 2024).

The spread of the injectate within the thoracolumbar fascia demonstrates the potential of the QL-Block to reach the abdominal sympathetic trunk (Garbin et al. 2020a; Garbin et al. 2020b; Viscasillas et al., 2021a; Alaman et al., 2022; Marchina-Gonçalves et al., 2022; Marchina-Gonçalves et al. 2023), potentially facilitating visceral analgesia. However, variations in the injection plane may affect the injectate's ability to effectively stain the sympathetic trunk (Marchina-Gonçalves et al. 2023).

Morphometric characteristics such as weight and body score are reported as factors that can increase the difficulty to performing the QL-Block injection, as they can hinder the formation of clear US images (Marchina-Gonçalves et al. 2023). Additionally, acoustic shadows created by bone structures (Viscasillas et al. 2021a)

can interfere with the visualization of part or all of the needle (Marchina-Gonçalves et al. 2023), further increasing the risk of complications *in vivo*.

In veterinary medicine, there is evidence that the QL-block may be useful for providing postoperative analgesia and managing abdominal pain caused by peritonitis. Two clinical trials evaluated its use at the L1 level for sterilization surgeries in female dogs (Viscasillas et al. 2021b; Degani et al. 2023), while two case series highlighted the use of epidural catheters in the QLP for interventional analgesia in canine patients with severe abdominal pain (Camargo-Fontanela et al. 2024; Degani et al. 2024).

The QL-Block shows promise for providing analgesia in dogs with severe abdominal pain. However, the optimal volume to use, the best injection approach, and the postoperative analgesic effects remain topics of ongoing discussion. This study aimed to compare dye spread in the QLP via IM or LL approaches using different volumes and to evaluate the influence of morphometric variables on the extent of dye spread in canine cadavers.

4.2 MATERIALS AND METHODS

4.2.1 Animals

A total of fifty-eight frozen (thawed within 72 hours before the study), refrigerated (removed from the refrigerator 12 hours prior to the study), or fresh cadavers (used within six hours of death) were used. The cadavers were obtained from partner veterinary clinics and hospitals, with deaths unrelated to the study. Cadavers showing any anatomical malformation, signs of trauma, or the presence of free intra-abdominal fluid were excluded. In our institution, approval from the Animal Ethics Committee is not required for cadaveric studies.

4.2.2 Ultrasound-guided injection

The injections of 0.1% methylene blue (Methylene Blue 0.1%; Farmax, MG, Brazil) were randomized between the IM or LL approaches, for volumes of 0.15, 0.3 and 0.6 mL kg^{-1}, forming the groups IM0.15, IM0.3, IM0. 6, LL0.15, LL0.3, LL0.6. All six groups participated in the randomization for each hemiabdomen an equal number of repetitions assigned to each treatment group (www.randomization.com). It was predetermined that each group should have a minimum of 18 successful repetitions, evenly distributed across three size categories: small (S), up to 10 kg; medium (M),

10.1–20 kg; and large (L), over 20 kg. This required at least six successful repetitions for each subgroup.

Data collected included breed, sex and morphometric parameters such as weight (kg), body condition score (1-9 scale) according to the WSAVA nutritional guidelines (Freeman et al. 2011), spinal length (measured in cm from the atlanto-occipital joint to the first coccygeal vertebra), thoracic circumference (measured in cm at the level of the eighth rib) and abdominal circumference (measured in cm at the level of the umbilical scar).

Prior to the study, the cadavers were extensively shaved in the bilateral laterodorsal thoracolumbar region and the skin was cleaned with alcohol. All injections were performed by the same researcher, who had four years' experience of US-guided regional blocks. Injection was performed first on the left side and once it was concluded, the procedure was repeated in the contralateral hemiabdomen.

A linear probe with a frequency of 5–12 Hz (MySono U6; LN5-12; MySono U6; LN5-12; Samsung Medison Co. LTD; Gangwon-do; Korea) was positioned caudal and parallel to the last rib, with the marker directed dorsally. This positioning allowed the acquisition of an US image of the region adjacent to the transverse process of L1, where the erector spinae muscle group, thoracolumbar fascia, and the QL and PM muscles were visible (Fig. 3A and 3B).

A Touhy needle (18G; 10 cm, BD Perisafe; Becton Dickinson, Brasil), attached to a 3-way stopcock connected to a dye syringe and an extension with a syringe filled with 0.9% saline solution, was introduced in-plane using a ventromedial IM or LL approach until its tip reached the desired injection point (Fig. 3C and 3D).

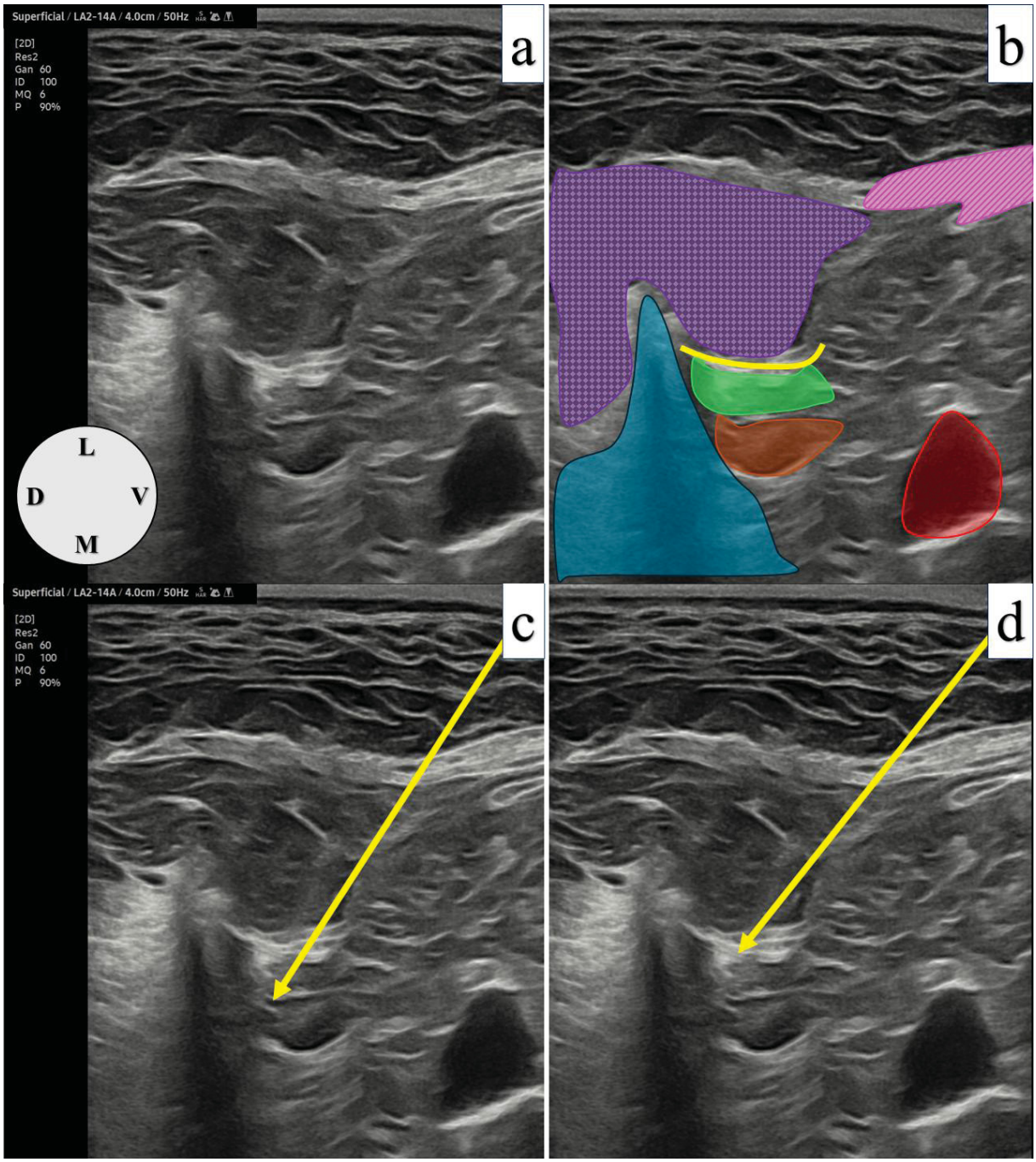

Figure 3 (A) Sonoanatomy image at the level of the first lumbar vertebra of a canine cadaver positioned in right lateral recumbency. (B) Structures highlighted: erector spinae muscle group in purple, transverse process of L1 in blue, quadratus lumborum muscle in green, psoas minor muscle in orange, thoracolumbar fascia represented by the yellow line, transversus abdominis plane in pink, and abdominal aorta in red. (C) Needle trajectory representation for the intermuscular approach to the quadratus lumborum plane. (D) Needle trajectory representation for the lateral lumbar approach to the quadratus lumborum plane.

A bolus of 0.1 mL of 0.9% saline was initially used to visualize hydrodissection of the structures comprising the QLP. Once the correct positioning of the needle tip was identified the total volume of dye for the IM or LL approach was administered.

The time to complete the injection technique was recorded, starting from probe contact with the skin until the complete administration of the dye. The quality of the images obtained during US-guided injection (Quality-I) was evaluated using adapted scores from Zoff et al. (2017):

- Visualization of QLP structures: 0 – Only the acoustic shadow of the L1 transverse process; 1 – The transverse process and thoracolumbar fascia; and 2 – The transverse process, thoracolumbar fascia, and QL and PM muscles.
- Needle projection visibility: 0 – Only the movement of structures adjacent to the needle; 1 – The needle body or tip; and 2 – Both the needle body and tip.
- Visualization of injected solution: 0 – No movement of QLP structures upon dye administration; 1 – Recognition of movement in adjacent structures upon dye administration (cascade effect); and 2 – Recognition of anechoic bubble formation due to hydrodissection of QLP upon dye injection.

4.2.3 Dissection

After the injection on the right hemiabdomen was completed, the cadavers were placed in dorsal recumbency and remained in this position until the dissection of both hemiabdomens was finished. As with the injections, the dissections always began on the left hemiabdomen. Fifteen minutes after the last injection, an initial incision was made along the ventral midline from the xiphoid to the pubis, followed by a second incision parallel to the caudal edge of the costal arch to expose the ventrolateral abdominal retroperitoneum. Any perforations in the peritoneum or organs were documented, and excess fat was removed to improve visualization of the hypaxial region, revealing the Pm and QL muscles along with the thoracolumbar ventral branches of spinal nerves (VBSN). The injection was considered successful when the dye was found adjacent to the quadratus lumborum muscle in the thoracolumbar interfascial plane and any excess was carefully removed with absorbent paper. The craniocaudal and dorsoventral spread of the dye was assessed through dissection and measured in centimeters.

Thoracolumbar nerves were dissected to assess successful dye staining. A nerve was considered stained if the dye was distributed over ≥1 cm of its circumference. Partial staining was defined as length <1 cm or incomplete circumferential staining. Failure was defined as no dye contacting the nerve (Fig. 4).

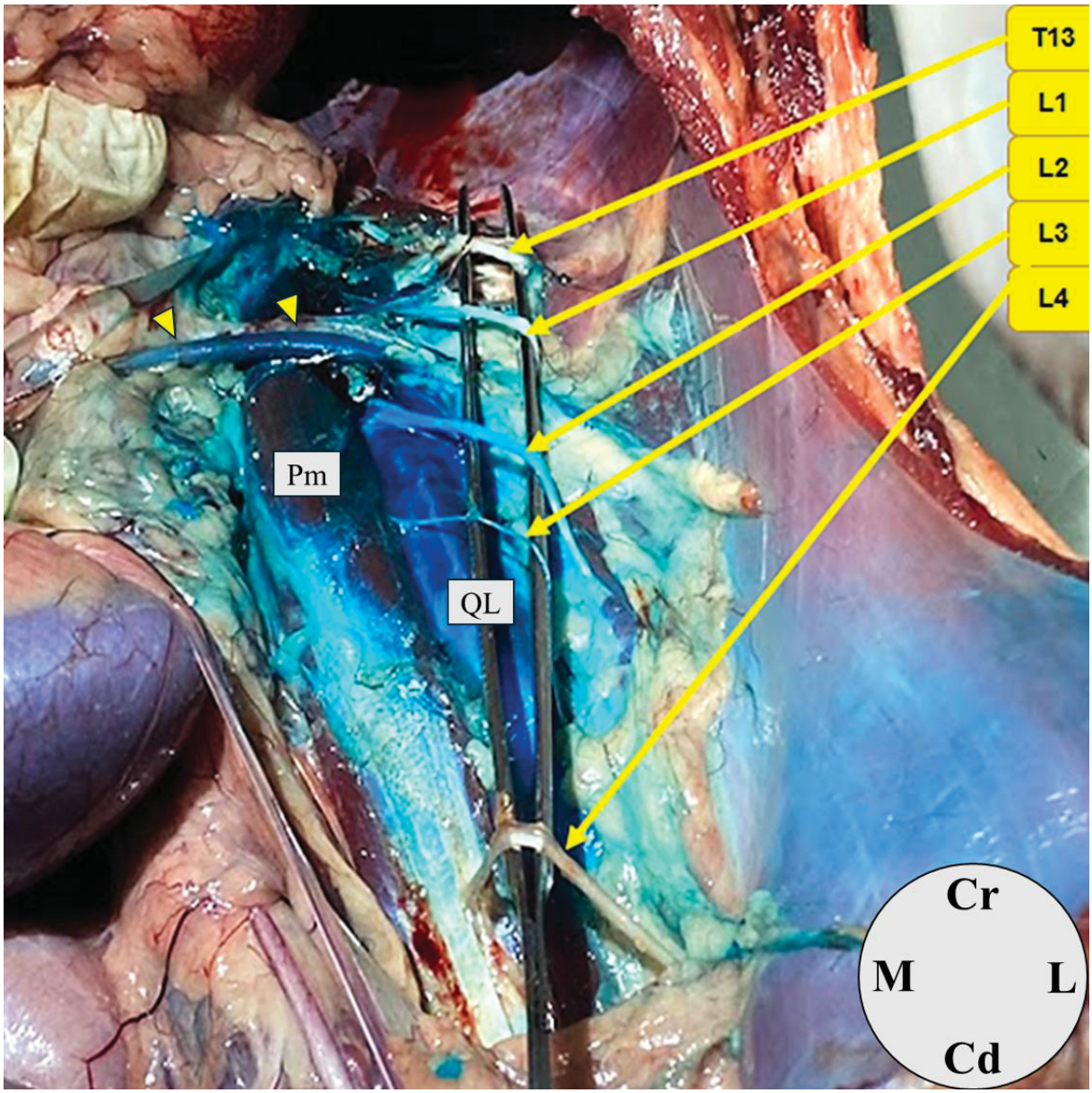

Figure 4. Visualization of the Quadratus Lumborum Plane (QLP) after dissecting the transversalis fascia through the retroperitoneum and removing excess fat in the left hemiabdomen of a canine cadaver with a body condition score of 3 (on a scale of 1–9), using a ventrolateral approach to the abdominal cavity. The ventral branches of the second (L2) and third (L3) lumbar spinal nerves were considered stained, the first (L1) lumbar ventral branch was partially stained, and the 13th thoracic (T13) and fourth lumbar (L4) branches were not stained. QL, quadratus lumborum muscle; Pm, psoas minor muscle; Yellow arrowhead, cranial abdominal vein.

For the left side, dissection time was recorded from the first contact of the scalpel with the skin to the documentation of dye impregnation and its craniocaudal and dorsoventral spread. For the right side, dissection time was recorded from the second paracostal incision to the documentation of dye impregnation and spread.

After assessing complications, dye spread, and stained VBSN, the nerves were bilaterally dissected along their paths toward their intervertebral foramina of origin to determine whether the foramina were stained. The Pm was also reflected to evaluate

staining of the sympathetic trunk, using the same success criteria as for the VBSN. These additional procedures were not included in the dissection time.

4.2.4 Statistical analysis

The number of repetitions required per group to determine differences in morphometric variables, Quality-I, and the success of sympathetic trunk staining was calculated for the Kruskal-Wallis or one-way ANOVA tests, with a desired power of 80% ($1-\beta = 0.8$) and a significance level of 0.05 ($\alpha = 0.05$). For weight, a mean difference of 2 kg and a standard deviation of 2 kg were assumed. For spinal length, thoracic circumference, and abdominal circumference, a mean difference of 5 cm and a standard deviation of 5 cm were assumed. For body condition score, a mean difference of 2 points and a standard deviation of 2 points were used. For Quality-I scores, a mean difference of 1 point and a standard deviation of 1 point were assumed. For the success of staining the sympathetic trunk, a mean difference of 1 success and a standard deviation of 1 success were used. The sample size required for morphometric variables was 10 repetitions per group, whereas for Quality-I and sympathetic trunk staining success, 16 repetitions were required. A total of 18 repetitions were performed per group (IM0.15, IM0.3, IM0.6, LL0.15, LL0.3, and LL0.6). For multiple regression and two-way ANOVA analyses evaluating craniocaudal spread, dorsoventral spread, and the number of stained VBSN, the power analysis was conducted based on the collected sample size. The multiple regression analysis showed a power of 0.93 ($1-\beta = 0.93$), with a significance level of 0.05 ($\alpha = 0.05$) and an effect size of 0.15 (Cohen, 1988). For the two-way ANOVA, the power was 80% ($1-\beta = 0.8$) with a significance level of 0.05 ($\alpha = 0.05$).

The collected data were tabulated in Excel spreadsheets (Microsoft Excel 2013; Microsoft Corporation, USA) and imported into statistical analysis software (SigmaPlot for Windows, version 12.0, Systat Software Inc., Germany). Data distribution was assessed using the Shapiro-Wilk test to distinguish between normal ($p > 0.05$) and non-normal samples ($p < 0.05$). Differences in morphometric data and the quality of US images between groups were analyzed using One-Way ANOVA for normally distributed data and Kruskal-Wallis tests for non-normally distributed data. Two distinct methods were applied to analyze the influence of approach, volume, and morphometric characteristics on dye spread and the number of stained VBSN: i) a two-factor analysis of variance (ANOVA) with Sidak's post-hoc analysis, considering only approach and

volume as factors; and ii) multiple linear regression, incorporating Stepwise techniques, to assess the effects of approach, volume, and morphometric characteristics.

4.3 RESULTS

Morphometric characteristics did not vary between the groups or approaches (Table 1 – in the Supplementary Material 3). The body condition scores, according to WSAVA nutritional guidelines (Freeman et al. 2011), classified the cadavers into nine under ideal (S = 5 / M = 2 / L = 2), 26 ideal (S = 8 / M = 10 / L = 8), and 23 over ideal (S = 7 / M = 6 / L = 10). Body condition scores showed a moderate positive Spearman correlation with abdominal circumference values ($\rho = 0.35$, $p < 0.01$). Body condition scores did not correlate with US visibility scores, although higher scores tended to interfere with the visualization of QLP structures (Fig. 5A). Additionally, abdominal circumference showed no correlation with QLP structure visibility scores.

The median time to perform the US-guided injection was 42 seconds (iqr 24.5), and the dissection time was 6.3 minutes (iqr 4.0), with no significant differences between groups. There were no significant differences between the scores of visualization of QLP structures, needle projection or visualization of injected solution among the groups.

The injection success rate was 94.7% (54/57) for the IM approach and 91.5% (54/59) for the LL approach. The technique was unsuccessful in eight hemiabdomens: three in the IM (one peritoneal perforation and two failures to penetrate the thoracolumbar fascia) and five in the LL approach (one peritoneal perforation, one renal fascia perforation and three failures to penetrate the thoracolumbar fascia). Of these, 75% (6/8) occurred in small animals and 25% (2/8) in large animals. All eight cases of technical errors occurred in cases with reduced Quality-I scores (7/8 Visualization of QLP structures and 1/8 Needle projection visibility).

The two-factor ANOVA revealed statistically significant differences across all three outcome variables: craniocaudal spread, dorsoventral spread, and the number of stained VBSN (Table 2 - in the Supplementary Material 3). The volume injected positively influences all three variables. The approach only influences the dorsoventral spread, with the LL approach showing greater spread. However, there was no significant interaction between the volume and the approach used.

Sidak's analyses showed a significant difference ($p < 0.0015$) in craniocaudal spread capacity across all volumes, demostrating a directly proportional increase with larger volumes (Fig. 5B). However, for the number of stained VBSN, a significant difference ($p < 0.0125$) was found only between the 0.15 mL kg^{-1} volume, which stained fewer VBSN, and the other volumes, with no significant differences between 0.3 and 0.6 mL kg^{-1} (Fig. 5C).

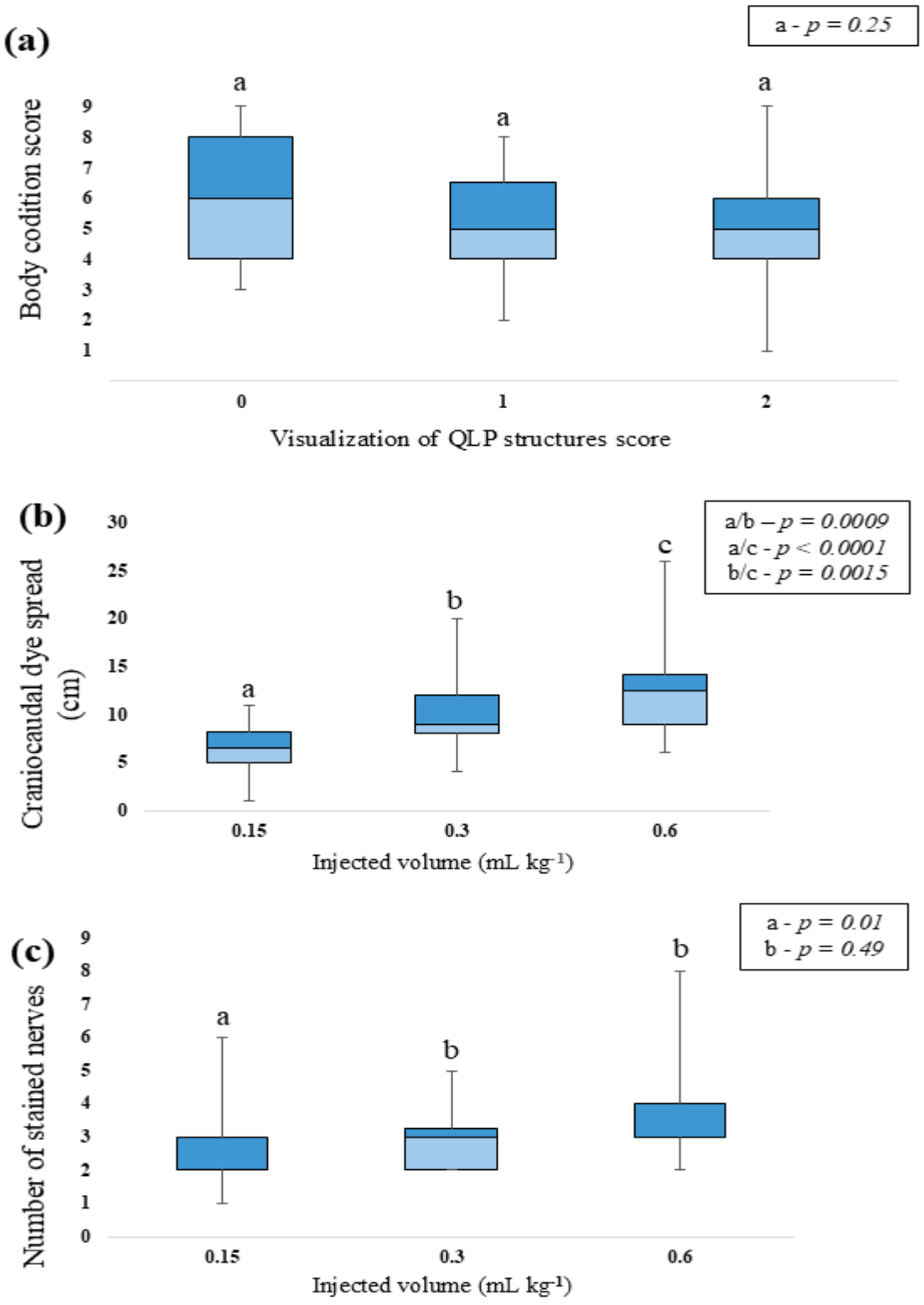

Figure 5. (A) Distribution of body condition score, according to WSAVA nutrition guidelines (Freeman et al. 2011), at different levels (2 - good, 1 - impaired, and 0 - poor) of quadratus lumborum plane (QLP) structure visualization in canine cadavers. (B) Craniocaudal dye spread in the QLP of canine cadavers with injected volumes of 0.15, 0.3, and 0.6 mL kg^{-1}. Different letters indicate significant differences between groups (Sidak test: $p < 0.0015$). (C) Stained ventral branches of spinal nerves distribution in the QLP of canine cadavers with injected volumes of 0.15, 0.3, and 0.6 mL kg^{-1}. Different letters indicate significant differences between groups (Sidak test: $p < 0.0125$).

For the multiple regression analysis, the following predictor variables were determined: approach (IM or LL), weight, spinal length, thoracic circumference, abdominal circumference, body score, scores for visualization of QLP structures, needle projection and visualization of injected solution. To avoid multicollinearity, Pearson and Spearman tests were used to remove variables with a high degree of correlation. Consequently, thoracic circumference and abdominal circumference were excluded from the models as they were correlated with each other ($r = 0.92$; $p < 0.05$) and strongly correlated with weight ($r = 0.94$ and $r = 0.92$, respectively; $p < 0.05$) and spinal length ($r = 0.85$ and $r = 0.75$, respectively; $p < 0.05$). The scores for visualization of QLP structures were also removed due to its correlation with the needle visualization scores ($r = 0.81$; $p < 0.005$). Additionally, weight and spinal length were highly correlated ($r = 0.85$; $p < 0.005$), leading to the creation of a combined variable: weight/length.

The final model for craniocaudal spread, following through the application of the Stepwise technique, included only the volume and the weight-to-spinal-length ratio as predictors. The model demonstrated an R^2 value of 0.448 ($p < 0.001$), signifying that these two variables collectively explain 45% of the variation in craniocaudal spread. The variables were ranked in terms of their relative importance as follows: volume (74.4%) and weight-to-spinal-length ratio (25.6%). Accordingly, the equation was established as: *"Craniocaudal spread = 1.52 + 13.54 (volume) + 14.15 (weight-to-spinal-length ratio)".*

The final model for dorsoventral spread, following the application of the Stepwise technique, incorporated only the approach (IM or LL), the volume, and the weight-to-spinal-length ratio. The model exhibited an R^2 value of 0.341 ($p < 0.001$), indicating that these three variables collectively account for 34% of the variation in dorso-ventral spread. The variables ranked in order of importance as follows: weight-to-spinal-length ratio (66.6%), volume (22.4%), and approach (11%). Accordingly, the equation was established as: *"Dorsoventral spread = 0.86 + 2.26 (volume) + 6.53 (weight-to-spinal-length ratio) + 0.53 (approach: IM = 0, LL = 1)".*

The final model for the number of stained VBSN, determined through the Stepwise technique, included only volume as a predictor. The model exhibited an R^2 value of 0.121 ($p < 0.001$), indicating that this variable accounts for 12% of the variation

in the number of stained VBSN. Accordingly, the following equation was established: *"Number of stained VBSN = 2.21 + 2.05 (volume)".* Furthermore, to evaluate the intrinsic influence of volume relative to the approach, a correlation analysis was conducted. The results demonstrated an R^2 value of 0.28 ($p = 0.031$) for IM and an R^2 value of 0.46 ($p = 0.001$) for LL.

In successful injections, the most frequently stained VBSN were L2, L3, and L1 for both IM and LL approaches, with no differences among groups. The T13 and L4 VBSN were stained at low frequencies, also without significant differences among groups (Fig. 6). Dye spread to the spinal foramen only in one hemiabdomen (S dog) in group IM0.6 mL kg^{-1}.

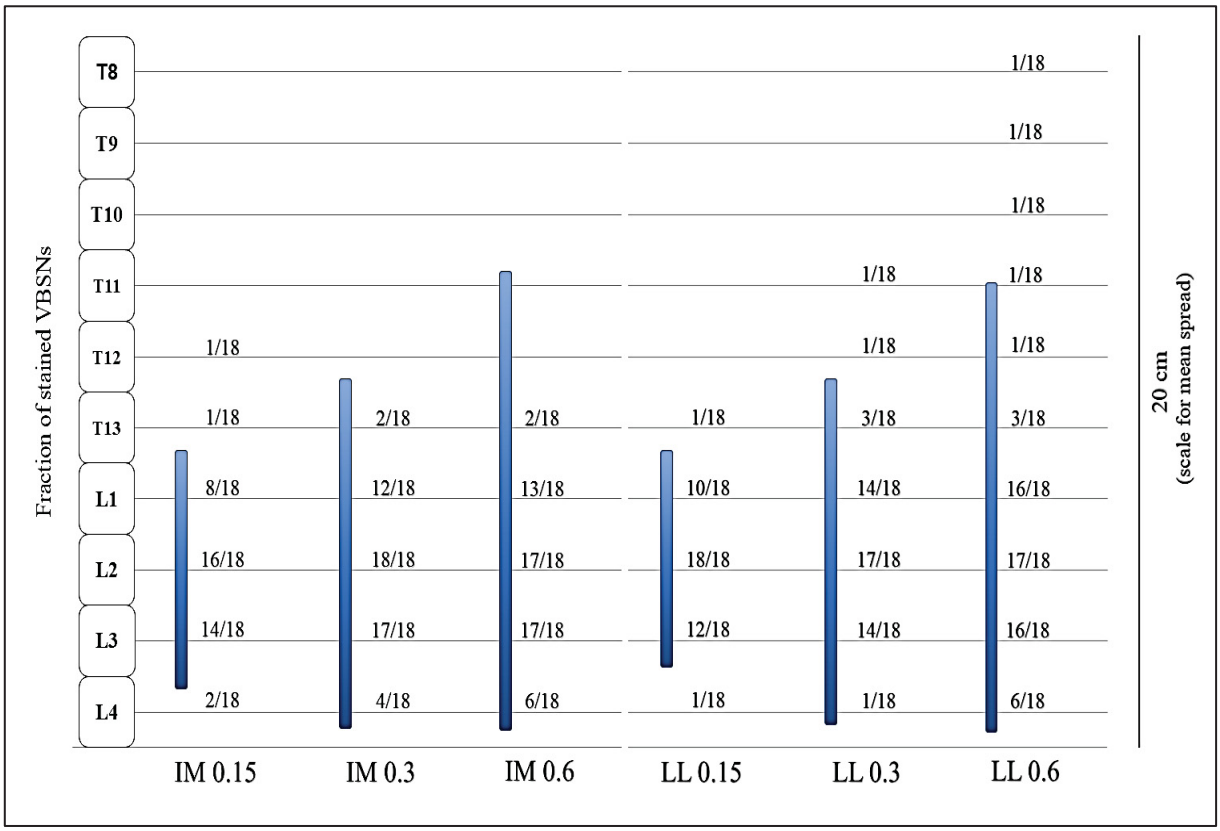

Figure 6. Representation of mean craniocaudal spread (blue bars) and the fraction of stained ventral branches of spinal nerves in the quadratus lumborum plane for the intermuscular (IM) and lateral lumbar (LL) approaches in canine cadavers with injected volumes of 0.15, 0.3, and 0.6 mL/kg in dogs cadavers. *Stars represent the fraction of ventral branches of nerve bundles from each spinal column segment outside the mean (respecting the total sample represented in the graph).

There was no significant difference in sympathetic trunk staining among groups and subgroups. The trunk was stained 14 times in IM (2, 3, and 9 for volumes of 0.15, 0.3, and 0.6, respectively) and eight times in LL (0, 4, and 4 for the volumes of 0.15, 0.3, and 0.6, respectively).

4.4 DISCUSSION

The morphometric distribution analysis revealed no significant differences between groups, suggesting data homogeneity that allowed for a more robust analysis of the injection techniques used.

Although Marchina-Gonçalves et al. (2023) suggested that the QL-Block injection may be more challenging to perform in larger or obese dogs, they did not find significant differences in the quality of US images. Similarly, Garbin et al. (2020) reported that visualizing the QL muscle may be more difficult in small dogs. However, these authors did not use a scoring system to assess the quality of US images of the QL structures but instead evaluated needle visualization, and they also did not find significant differences. Consistent with these findings, the present study found no significant differences in the visualization scores of QLP structures, needle projection, or injected solution among the groups. However, a trend was observed indicating that dogs with higher body condition scores tended to have lower visualization scores for QLP structures.

As observed in previous studies, the injection success rates were high in both IM and LL approaches, with technique failures occurring in small or large cadavers when the visibility of structures or the needle was impaired. Marchina-Gonçalves et al. (2023), recommended ensuring optimal needle tip visibility for QL-Block in live animals. They also suggested that if imaging at the L1 level proves difficult, it may be prudent to consider alternative blocks with potentially greater accuracy and fewer errors. Those findings suggest that image quality scores do not correlate with the ease of performing the QL-Block in dogs. However, low scores may be associated to technique failure and complications, as previously reported for the transverse abdominal plane block by Zoff et al. (2019).

The IM and LL approaches were selected as they represent medial and lateral approaches to the QLP. The results suggest that these approaches are similar in terms of spread capacity and thoracolumbar nerve staining for each corresponding volume, findings consistent with Marchina-Gonçalves et al. (2023). Conventionally, spread data for the QL-Block injection are reported as the number of vertebrae or stained nerve branches (Garbin et al. 2020a; Garbin et al. 2020b; Viscasillas et al. 2021a; Viscasillas et al. 2021b; Alaman et al. 2022; Marchina-Gonçalves et al. 2022; Marchina-Gonçalves et al. 2023; Degani et al. 2024). However, in the present study, spread was analyzed

also based on craniocaudal and dorsoventral dimensions in cm, with a distinct analysis performed for the number of stained VBSN.

The fact that the dorsoventral spread of the dye was greater in the LL groups can be explained by the distribution of the dye between the thoracolumbar fascia and the transversalis fascia. However, this finding does not seem to have clinical relevance, as it did not influence the number of stained VBSN, the sympathetic trunk staining, or the incidence of complications.

In different cadaveric studies in dogs, it has been suggested that larger injectate volumes tend to stain more nerve branches; however, these differences did not reach statistical significance (Garbin et al. 2020; Viscasillas et al. 2021; Alaman et al. 2022; Marchina-Gonçalves et al. 2023). These studies also indicate that although larger volumes are associated with greater spread along the spinal segments, they do not necessarily stain a greater number of nerve branches (Viscasillas et al. 2021; Marchina-Gonçalves et al. 2022). In the present study, it was also observed that larger volumes resulted in greater craniocaudal dye spread. However, unlike previous studies, larger volumes in this study were associated with a significantly greater number of stained nerve branches. With volumes of 0.3 mL kg^{-1} and 0.6 mL kg^{-1}, significantly more VBSN were stained compared to 0.15 mL kg^{-1}. No differences were observed between 0.3 and 0.6 mL kg^{-1}, indicating that using volumes above 0.3 mL kg^{-1} offers no additional advantages.

The weight-to-spinal length ratio was identified as the second most influential variable for craniocaudal spread and the most influential for dorsoventral spread. These results are plausibly associated with the proportional increase in thoracolumbar fascia length in larger and more elongated animals. On the other hand, when evaluating the influence of this morphometric variable on the number of stained nerve bundles, no significant correlation was observed.

Marchina-Gonçalves et al. (2023) propose that positioning the needle tip closer to the vertebral body may achieve a broader spread of the injected solution. A weak correlation was observed between the volume and the number of stained VBSN for the IM approach, while a strong correlation was found for the LL approach. This observed effect is likely due to the anatomical arrangement of the structures within the QLP, which appears to allow a more homogeneous spread with the IM approach.

L1, L2, and L3 were the most frequently stained VBSN, consistent with the literature (Garbin et al., 2020a; Viscasillas et al., 2021; Marchina-Gonçalves et al.,

2023). Larger volumes and IM more frequently stained T13 and L4, as also reported by Marchina-Gonçalves et al. (2023). However, no study has demonstrated significant differences in the number of stained VBSN with increased volumes.

The correlation analysis indicated that the number of stained VBSN is influenced solely by the volume across the collected variables and approaches. However, the mathematical model derived from the correlation accounts for only 12% of the variation in the number of stained VBSN. These findings suggest that the standard spread of the QL block is primarily limited to the first three lumbar nerve branches and that cranial or caudal gains may depend heavily on operator-related factors or other unconsidered variables.

The dye reached the intervertebral foramina and the sympathetic trunk more frequently with the IM approach and larger volumes, although the occurrences were too few to demonstrate significant differences. Regarding the sympathetic trunk, Marchina-Gonçalves et al. (2023) reported a similar number of dye impregnations, while Garbin et al. (2020a) and Garbin et al. (2020b) observed more frequent successes, and Alaman et al. (2022) found significant differences for the dorsal approach with larger volumes. These findings suggest the potential for greater homogeneity in dye spread to the sympathetic trunk with approaches closer to the vertebral body and highlight the intrinsic role of the operator in ensuring the quality of solution spread within the QLP.

This study has some limitations due to the use of cadavers in three different conditions (frozen, refrigerated, and fresh), which may have influenced image quality and dye diffusion. All injections and dissections were performed by the same evaluator, introducing potential bias. Spinal canals were not dissected to assess intramedullary dye spread; however, only one case reached the intervertebral foramina. The investigator's prior experience with *in vivo* QL-Block may have affected the assessment of image quality and technical difficulty. The use of a single needle size may also impact proper fascial puncture, particularly in small animals.

4.5 CONCLUSION

The IM and LL approaches provided adequate distribution over the main nerve bundles for analgesia in caudal abdominal surgeries and appear to be equivalent in terms of craniocaudal spread and the number of VBSN stained and staining of the sympathetic trunk. The increase in volume appears to directly influence craniocaudal

spread, but volumes exceeding 0.3 mL kg^{-1} do not increase the number of stained VBSN. Morphometric variables appear to influence both craniocaudal and dorsoventral spread capacity but do not affect the number of stained VBSN.

**Images of cadaver positioning, incision lines for dissection, and technical error are found in Supplementary Material 4.

5 – PRELIMINARY VALIDATION OF A MATHEMATICAL MODEL FOR PREDICTING INDIVIDUAL INJECTATE VOLUME IN THE QUADRATUS LUMBORUM PLANE IN DOGS

5.1 INTRODUTION

Dogs exhibit considerable anatomical variability among individuals, one of which relates to the axial skeleton length. Regional blocks that rely on craniocaudal spread may be influenced by these variations. Individualizing the required volume to achieve the proper craniocaudal spread of anesthetic solutions can ensure greater block efficacy, while respecting the necessary dose for each body type (Tayary et al. 2022).

5.2 MATERIALS AND METHODS

5.2.1 Animals

A total of six cadavers were used, either refrigerated (removed from refrigeration 12 hours before the study) or fresh (used within six hours post-mortem). The cadavers were obtained from partner veterinary clinics and hospitals, with deaths unrelated to the study. Cadavers presenting any anatomical malformations, signs of trauma, or intra-abdominal fluid presence were excluded. At our institution, approval from the Animal Ethics Committee is not required for cadaveric studies.

5.2.2 Ultrasound-guided injection

The 0.1% methylene blue injections (Methylene blue 0.1%, Farmax, MG, Brazil) were performed using the IM approach and were randomized to determine the calculation method for the injected volume in each hemiabdomen. The assigned methods included either the previously described formula for craniocaudal spread (formula group) or a pre-fixed volume of 0.3 mL kg^{-1} (control group). Each cadaver received both approaches, with one applied to each hemiaabdomen, following a randomization process (www.randomization.com).

Collected data included breed, sex, and morphometric parameters, such as weight and ideal weight (kg), body condition score (on a 1 to 9 scale, based on WSAVA nutritional guidelines) (Freeman et al. 2011), vertebral column length (measured in cm

from the atlanto-occipital joint to the first coccygeal vertebra), and lumbar column length (measured from the head of the last rib to the ilium wing).

The formula application method aimed to achieve spread covering the vertebral bodies of the first four lumbar vertebrae, excluding cranial spread, corresponding to approximately 60% of the lumbar column length (Lacowicz et al. 2024). The formula was adjusted to use volume as a variable (mL kg^{-1}), maintaining the following equation, using the ideal weight.:

$$\text{Volume} = \frac{\left(\left(\frac{\text{weight}}{\text{vertebral column length}}\right) \times -14.15 - 1.52 + (\text{lumbar column length} \times 0.6)\right)}{13.54}$$

The cadaver preparation, ultrasound imaging technique, final needle positioning in the IM approach, dissection, and assessment of dye spread over the VBSN were carried out strictly following the methodology described in the previous chapter of this thesis

5.3 RESULTS

The median time to perform the US-guided injection was 40 seconds (IQR 15.6), and the dissection time was 8.4 minutes (IQR 3.7). The mean vertebral column length was 54.8± 9.5 cm, the mean body weight was 9.9 ± 4.6 kg, the mean lumbar column length was 13.8 ± 1.5 cm, and the median body condition score was 5 (IQR 3.5). The volume for the formula group was 0.3 ± 0.1 mL kg^{-1}.

The injection success rate was 100% (6/6) for the IM approach in both the formula group and the control group. The craniocaudal spread was 8.7 ± 1.6 cm and 9.4 ± 2.4 cm for the formula and control groups, respectively. The expected craniocaudal spread in the formula group was 60% of the measured lumbar column length, with an average error of 0.6 cm (approximately 10%) between the estimated and collected values.

The VBSN L2 and L3 were stained in all repetitions for both groups, except in one cadaver, which lacked the bilateral ventral branch of L3. The VBSN L1 was not stained in only one repetition in the control group. T13 was stained three times in the formula group and once in the control group. The sympathetic trunk was stained five times in the formula group and three times in the control group (Figure 7).

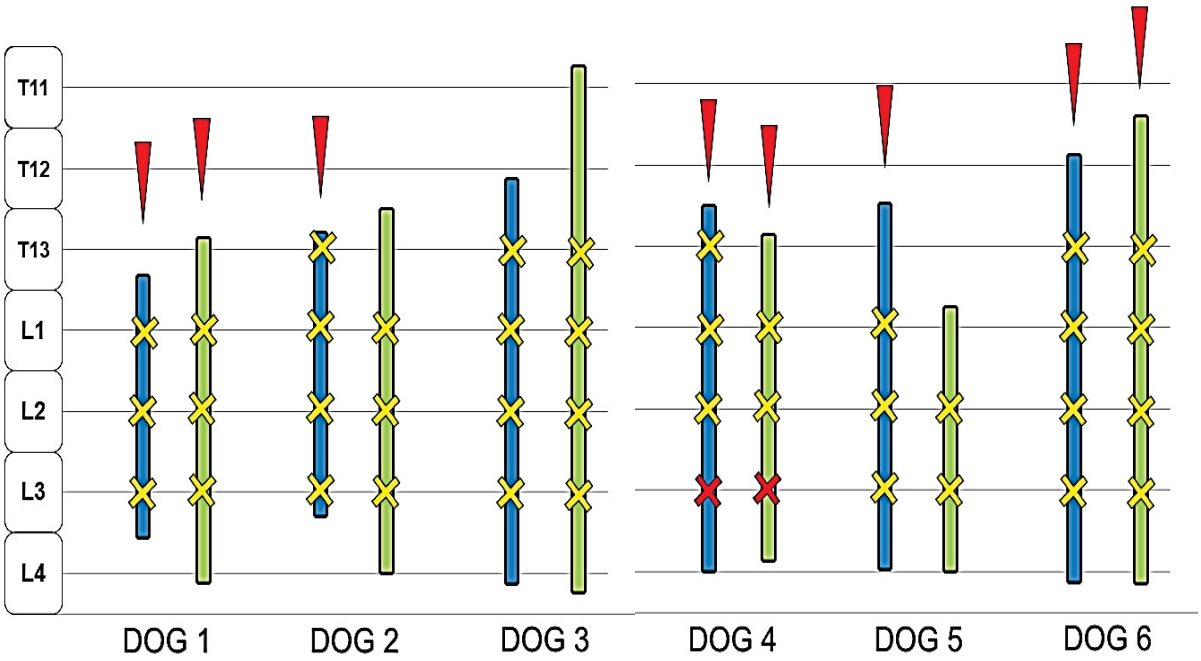

Figure 7. Representation of craniocaudal spread for the formula group (blue bars) and control group (green bars). Respective stained nerves (yellow X's), stained sympathetic trunk (red arrowheads), and absence of the ventral branch due to anatomical variation (red X's).

5.4 DISCUSSION

The craniocaudal spread was slightly greater in the control group, while the formula group stained a slightly higher number of nerves and the sympathetic trunk. The most commonly stained nerves were L1, L2, and L3, consistent with descriptions in the literature (Garbin et al., 2020a; Viscasillas et al., 2021; Marchina-Gonçalves et al., 2023). The sympathetic trunk staining rate was considerable (8/12), possibly due to the choice of the IM approach, which is closer to the vertebral body (Marchina-Gonçalves et al., 2023).

The formula group stained slightly more VBSN. Tayary et al. (2022) reported that a method used to calculate the volume for epidural anesthesia in dogs, based solely on body weight, may underestimate or overestimate the required volume. These findings reinforce that in techniques requiring craniocaudal spread, volumes based on vertebral column length may be predictors of success.

The mean volume for the formula group was 0.3 mL kg^{-1}, with variations between 0.2 and 0.4 mL kg^{-1}. In the literature, volumes starting from 0.2 mL kg^{-1} have been effective in staining the thoracolumbar VBSN (Viscasillas et al., 2021a). However, an increase in volume leads to wider spread of the injectate (Marchina-Gonçalves et

al., 2023). Our study on morphometric variables (Chapter 4) demonstrated that greater craniocaudal spread does not necessarily result in a higher number of stained nerves. This effect may have been observed due to the lack of volume individualization based on the animal's morphometry and the absence of a defined craniocaudal spread threshold required to stain at least the first three lumbar VBSN.

Procedures such as total mastectomy may require regional anesthesia interventions involving multiple blocks (Portela et al. 2014, Teixeira et al. 2018). Individualizing the injectate volume administered in each block can benefit dogs that require lower volumes relative to body mass, ensuring the desired craniocaudal spread without reaching toxic doses.

This chapter represents the preliminary phase of a study aimed at individualizing the injectate volume in the QLP of dogs. Multicentric trials involving different technique operators are necessary to validate the developed equation. The results may present bias, as they were performed by the same operator who developed the formula. Dogs with significant alterations in the weight-to-spine length ratio, such as very small dogs, or those with free fluid or extensive neoplasms, may exhibit higher bias when using the formula.

5.5 CONCLUSION

The proposed equation demonstrates potential for individualizing the injectate volume for QL-Block in dogs. However, multicentric studies involving different operators and a greater heterogeneity of animals are necessary to validate the equation with greater accuracy.

6 CONCLUSIONS

The use of a catheter in the QLP for intermittent analgesia appears to provide benefits as part of a multimodal pain management protocol in dogs with peritonitis. The IM and LL approaches show similar efficacy for QL-Block at the L1 level, and an increase in craniocaudal spread does not necessarily result in a greater number of stained nerves. The proposed equation demonstrates potential for individualizing the injectate volume for QL-Block in dogs.

6.1 RECOMMENDATIONS FOR FUTURE STUDIES

The use of catheters for continuous analgesia in the QLP in randomized clinical trials to determine the feasibility of prolonged application of this technique in dogs. Future studies should evaluate possible associated complications, the optimal catheter retention time, and comparisons with conventional analgesia techniques.

Conducting clinical trials in dogs to assess the efficacy of QL-Block, comparing it to other locoregional blocks or analgesic infusions in abdominal cavity surgical procedures and peritonitis cases. These studies should include postoperative pain response monitoring and the need for supplemental analgesia. Additionally, comparisons of different types, concentrations, and duration of local anesthetic blocks in the QLP should be conducted.

Determining the optimal and individualized anesthetic volume for each dog, based on morphometric characteristics, to maximize the success of spread among operators.

REFERENCES

AFRIDI, B.; KHAN, H.; AKKOL, E. K.; ASCHNER, M. Pain perception and management: Where do we stand? **Current Molecular Pharmacology**, v. 14, n. 5, p. 678–688, 2021. DOI: 10.2174/1874467213666200611142438.

ALAMAN, M.; BONASTRE, C.; BLAS, I. et al. Description of a novel ultrasound-guided approach for a dorsal quadratus lumborum block: a canine cadaver study. **Veterinary Anaesthesia and Analgesia**, v. 49, n. 1, p. 118-125, 2022. DOI: 10.1016/j.vaa.2021.09.002.

ANDRADE, S. F.; FANTONI, D. T.; CORTOPASSI, S. R. G.; NETO, J. P. A.; KANASHIRO, G. P. Terapêutica do sistema nervoso. In: ANDRADE, S. F. **Manual de Terapêutica Veterinária**. 3. ed. Rio de Janeiro: Roca, 2008. Cap. 17, p. 97-114.

BARFIELD, D. M.; TIVERS, M. S.; HOLAHAN, M.; WELCH, K.; HOUSE, A.; ADAMANTOS, S. E. Retrospective evaluation of recurrent secondary septic peritonitis in dogs (2000–2011): 41 cases. **Journal of Veterinary Emergency and Critical Care**, v. 26, n. 2, p. 281–287, 2016. DOI: 10.1111/vec.12413.

BARRY, G.; SEHMBI, H.; RETTER, S.; BAILEY, J. G.; TABLANTE, R.; UPPAL, V. Comparative efficacy and safety of non-neuraxial analgesic techniques for midline laparotomy: a systematic review and frequentist network meta-analysis of randomised controlled trials. **PAIN**, v. 131, n. 6, p. 1053-1071, 2023. DOI: 10.1016/j.bja.2023.08.024

BUDRAS, K.; MCCARTHY, P. H.; FRICKE, W.; RICHTER, R.; HOROWITZ, A.; BERG, R. **Anatomia do Cão**. 5. ed. Barueri: Editora Manole, 2012. p. 219.

CAMARGO-FONTANELA, M. A.; KLAUMANN, P. R.; PIONTKOVSKY, R. J. et al. Preliminary experience with quadratus lumborum catheters for intermittent analgesia in three dogs with acute abdominal pain**. Veterinary Anaesthesia and Analgesia**, v. 51, n. 5, p. 575-578, 2024. DOI: 10.1016/j.vaa.2024.05.010.

CASTAÑEDA-HERRERA, F. E.; BURITICÁ-GAVIRIA, E. F.; ECHEVERRY-BONILLA, D. F. Anatomical evaluation of the thoracolumbar nerves related to the transversus abdominis plane block technique in the dog. **Anatomia, Histologia, Embryologia**, v. 46, n. 4, p. 373-377, ago. 2017. DOI: 10.1111/ahe.12279.

CHIN, K. J.; LIRK, P.; HOLLMANN, M. W.; SCHWARZ, S. K. W. Mechanisms of action of fascial plane blocks: a narrative review. **Regional Anesthesia & Pain Medicine**, v. 46, n. 7, p. 618-628, 2021. DOI: 10.1136/rapm-2020-102305.

COHEN, J. **Statistical Power Analysis for the Behavioral Sciences**. 2nd ed. Hillsdale, NJ: Lawrence Erlbaum Associates, 1988.

DEGANI, M.; BOLEN, G.; TALARICO, C.; NOËL, S.; GOMMEREN, K.; DI FRANCO, C.; SANDERSEN, C. Description and outcomes of an ultrasound-guided technique for catheter placement in the canine quadratus lumborum plane: A cadaveric tomographic study and clinical case series. **Veterinary Sciences**, v. 11, p. 472, 2024. DOI: 10.3390/vetsci11100472.

DEGANI, M.; DI FRANCO, C.; TAYARI, H.; FAGES CARCÉLES, A.; FIGÀ TALAMANCA, G.; SANDERSEN, C.; BRIGANTI, A. Postoperative analgesic effect of bilateral quadratus lumborum block (QLB) for canine laparoscopic ovariectomy: comparison of two concentrations of ropivacaine. **Animals**, v. 13, n. 23, p. 3604, 2023. DOI: 10.3390/ani13233604.

ELSHARKAWY, H.; EL-BOGDHADLY, K.; BARRINGTON, M. Quadratus Lumborum Block. Anesthesiology, v. 130, n. 2, p. 322–335, 2019. DOI: 10.1097/ALN.0000000000002524.

EVANS, H. E.; LAHUNTA, A. The autonomic nervous system. In: EVANS, H. E.; LAHUNTA, A. **Miller's Anatomy of the Dog**. 4. ed. St. Louis: Elsevier, 2013. Cap. 15, p. 575-785.

FREEMAN, L.; BECVAROVA, I.; CAVE, N. et al. WSAVA Guidelines for Nutritional Assessment. **Journal of Small Animal Practice**, 2011. DOI: 10.1111/j.1748-5827.2011.01079.x.

FREITAG, F. A. V.; BOZAK, V. L.; DO CARMO, M. P. W.; FROES, T. R.; DUQUE, J. C. M. Continuous transverse abdominal plane block for analgesia in three dogs with abdominal pain. **Veterinary Anaesthesia and Analgesia**, v. 45, n. 6, p. 1-3, 2018. DOI: 10.1016/j.vaa.2018.02.003.

FREITAG, F. A. V.; GAIO, T. S.; DOS SANTOS, A. A. M.; MUEHLBAUER, E.; MACHADO, M.; DUQUE, J. C. M. Ultrasound-guided superficial serratus plane block in dog cadavers: an anatomical evaluation and volume dispersion study. **Veterinary Anaesthesia and Analgesia**, v. 47, n. 1, p. 88-94, 2020. DOI: 10.1016/j.vaa.2019.08.003.

FREITAG, F. A. V.; MUEHLBAUER, E.; GAIO, T. D.; DOS SANTOS, A. A. M.; MACHADO, M.; SANCHEZ, A.; DUQUE, J. C. M. Evaluation of injection volumes for the transversus abdominis plane block in dog cadavers: a preliminary trial. **Veterinary Anaesthesia and Analgesia**, v. 48, n. 1, p. 142-146, 2021. DOI: 10.1016/j.vaa.2020.10.001.

GAO, T.; WANG, Y.; ZHENG, Y.; YU, Y.; LI, Q.; ZHANG, L. Quadratus lumborum block vs. transversus abdominis plane block for postoperative pain control in patients with nephrectomy: a systematic review and network meta-analysis. **Journal of Clinical Anesthesia**, v. 95, art. 111453, 2024. DOI: 10.1016/j.jclinane.2024.111453.

GARBIN, M.; PORTELA, D. A.; BERTOLIZIO, G.; GALLASTEGUI, A.; OTERO, P. E. A novel ultrasound-guided lateral quadratus lumborum block in dogs: a comparative cadaveric study of two approaches. **Veterinary Anaesthesia and Analgesia**, v. 47, n. 6, p. 810-818, 2020b. DOI: 10.1016/j.vaa.2020.08.003.

GARBIN, M.; PORTELA, D. A.; BERTOLIZIO, G.; GARCIA-PEREIRA, F.; GALLASTEGUI, A.; OTERO, P. E. Description of ultrasound-guided quadratus lumborum block technique and evaluation of injectate spread in canine cadavers.

Veterinary Anaesthesia and Analgesia, v. 47, n. 2, p. 249-258, 2020a. DOI: 10.1016/j.vaa.2019.12.005.

GARCIA, E. R. Anestésicos locais. In: GRIMM, K. A.; LAMONT, L. A.; TRANQUILLI, W. J.; GREENE, S. A.; ROBERTSON, S. A. **Lumb & Jones: Anestesiologia e Analgesia em Veterinária**. Rio de Janeiro: Guanabara Koogan, 2017. Cap. 17.

GRUNDY, L.; ERICKSON, A.; BRIERLEY, S. M. Visceral pain. **Annual Review of Physiology**, v. 81, p. 261–284, 2019. DOI: 10.1146/annurev-physiol-020518-114525.

HALL, J. E.; GUYTON, A. C. Sensações somáticas: II. Dor, cefaleia e sensações térmicas. In: HALL, J. E.; GUYTON, A. C. **Hall e Guyton Tratado de Fisiologia** Médica. Rio de Janeiro: Elsevier, 2011. Cap. 48, p. 617-630.

HERMANSON, J. W. The Muscular System. In: HERMANSON, J. W.; DE LAHUNTA, A.; EVANS, H. E**. Miller and Evans' Anatomy of the Dog**. 5. ed. St. Louis: Elsevier, 2020. Cap. 15, p. 444-658. ISBN: 9780323546027.

HERMANSON, J. W.; DE LAHUNTA, A.; EVANS, H. E. The Skeleton. In: HERMANSON, J. W.; DE LAHUNTA, A.; EVANS, H. E**. Miller and Evans' Anatomy of the Dog**. 5. ed. St. Louis: Elsevier, 2020a. Cap. 15, p. 182-374. ISBN: 9780323546027.

HERMANSON, J. W.; DE LAHUNTA, A.; EVANS, H. E. The Heart and Arteries. In: HERMANSON, J. W.; DE LAHUNTA, A.; EVANS, H. E**. Miller and Evans' Anatomy of the Dog**. 5. ed. St. Louis: Elsevier, 2020b. Cap. 15, p. 1015-1169. ISBN: 9780323546027.

HERMANSON, J. W.; DE LAHUNTA, A.; EVANS, H. E. The Veins. In: HERMANSON, J. W.; DE LAHUNTA, A.; EVANS, H. E**. Miller and Evans' Anatomy of the Dog**. 5. ed. St. Louis: Elsevier, 2020c. Cap. 15, p. 1170-1227. ISBN: 9780323546027.

HERMANSON, J. W.; DE LAHUNTA, A.; EVANS, H. E. The Spinal Nerves. In: HERMANSON, J. W.; DE LAHUNTA, A.; EVANS, H. E**. Miller and Evans' Anatomy**

of the Dog. 5. ed. St. Louis: Elsevier, 2020d. Cap. 15, p. 1407-1500. ISBN: 9780323546027.

KÖNIG, H. E.; LIEBICH, H. Órgãos genitais femininos. In: KÖNIG, H. E.; LIEBICH, H. **Anatomia dos Animais Domésticos**. Porto Alegre: Artmed, 2012. Cap. 12, p. 443-460.

LACOWICZ, C.; MACIEL, J.V.B.; FERNANDES, A.; FERREIRA, A.A.; DORNBUSCH, P.T. Comparative ex vivo morphometric tomographic study of lumbar spine between dog and rabbit. **Arquivo Brasileiro de Medicina Veterinária e Zootecnia**, Belo Horizonte, v. 76, n. 1, p. 16-22, 2024. DOI: 10.1590/1678-4162-12979.

LECLEZIO, L.; JANSEN, A.; WHITTEMORE, V. H. et al. Pilot validation of the Tuberous Sclerosis-Associated Neuropsychiatric Disorders (TAND) checklist. **Pediatric Neurology**, v. 52, n. 1, p. 16-24, 2014. DOI: 10.1016/j.pediatrneurol.2014.10.006.

LIU, X.; SONG, T.; CHEN, X.; ZHANG, J.; SHAN, C.; CHANG, L.; XU, H. Quadratus lumborum block versus transversus abdominis plane block for postoperative analgesia in patients undergoing abdominal surgeries: a systematic review and meta-analysis of randomized controlled trials. **BMC Anesthesiology**, v. 20, art. 53, 2020. DOI: 10.1186/s12871-020-00967-2

MARCHINA-GONÇALVES, A.; GIL, F.; LAREDO, F. G.; SOLER, M.; AGUT, A.; BELDA, E. Evaluation of high-volume injections using a modified dorsal quadratus lumborum block approach in canine cadavers. **Animals (Basel)**, v. 12, n. 1, p. 18, 2022. DOI: 10.3390/ani12010018.

MARCHINA-GONÇALVES, A.; LAREDO, F. G.; GIL, F.; SOLER, M.; AGUT, A.; REDONDO, J. I.; BELDA, E. An ultrasound-guided latero-ventral approach to perform the quadratus lumborum block in dog cadavers. **Animals**, v. 13, n. 13, p. 2214, 2023. DOI: 10.3390/ani13132214.

MIGUEL-GARCIA, C.; WHYTE, M.; ST JAMES, M.; FERREIRA, T. H. Effect of contrast and local anesthetic on dye spread following transversus abdominis plane injection in dog cadavers. **Veterinary Anaesthesia and Analgesia**, v. 47, n. 3, p. 391-395, 2020. DOI: 10.1016/j.vaa.2020.01.003.

PORTELA, D. A.; ROMANO, M.; BRIGANTI, Â. Avaliação clínica retrospectiva do bloqueio do plano transverso do abdome guiado por ultrassom em cadelas submetidas à mastectomia. **Veterinary Anaesthesia and Analgesia**, v. 41, n. 3, p. 319-324, maio 2014. DOI: 10.1111/vaa.12122.

POOLEY, R.; VENEZIANO, G.; BURRIER, C.; TRAM, N. K.; TOBIAS, J. D. Preliminary experience with quadratus lumborum catheters for postoperative pain management in pediatric-aged patients with contraindications to epidural anesthesia. **Journal of Clinical Medical Research**, v. 14, n. 10, p. 425-431, 2022. DOI: 10.14740/jocmr4813.

REID, J.; NOLAN, A. M.; HUGHES, L.; LASCELLES, B. D. X. Development of the short-form Glasgow Composite Measure Pain Scale (CMPS-SF) and derivation of an analgesic intervention score. **Animal Welfare**, v. 16, n. 1, p. 97-104, 2007. DOI: 10.1017/S096272860003178X.

SOLOMON, S. B.; BANKS, S. M.; GERSTENBERGER, E.; CSAKO, G.; BACHER, J. D.; THOMAS III, M. L.; COSTELLO, R.; EICHACKER, P. Q.; DANNER, R. L.; NATANSON, C. Sympathetic blockade in a canine model of gram-negative bacterial peritonitis. **Shock**, v. 19, n. 3, p. 215–222, 2003. DOI: 10.1097/00024382-200303000-00004

SPACKMAN, D. R.; MCLEOD, A. D. M.; PRINEAS, S. N.; LEACH, R. M.; REYNOLDS, F. Effect of epidural blockade on indicators of splanchnic perfusion and gut function in critically ill patients with peritonitis: a randomised comparison of epidural bupivacaine with systemic morphine. **Intensive Care Medicine**, v. 26, p. 1638-1645, 2000. DOI: 10.1007/s001340000671.

TAYARI, H.; OTERO, P. E.; D'AGOSTINO, M.; BARTOLINI, F.; BRIGANTI, A. Epidural volume of injectate using a dose regimen based on occipito-coccygeal spinal length

(OCL): randomized clinical study comparing different ropivacaine concentrations, with or without morphine, in bitches undergoing total unilateral mastectomy. **Animals**, v. 12, p. 587, 2022. DOI: 10.3390/ani12050587.

TEIXEIRA, L. G.; PUJOL, D. M.; PAZZIM, A. F.; SOUZA, R. P.; FADEL, L. Combination of transversus abdominis plane block and serratus plane block anesthesia in dogs submitted to mastectomy. **Pesquisa Veterinária Brasileira**, v. 38, n. 2, fev. 2018. DOI: 10.1590/1678-5150-PVB-5007.

VISCASILLAS, J.; SANCHIS-MORA, S.; BURILLO, P.; ESTEVE, V.; DEL ROMERO, A.; LAFUENTE, P.; REDONDO, J. I. Evaluation of quadratus lumborum block as part of an opioid-free anaesthesia for canine ovariohysterectomy. **Animals (Basel)**, v. 11, n. 12, p. 3424, 2021. DOI: 10.3390/ani11123424.

VISCASILLAS, J.; TERRADO, J.; MARTÍ-SCHARFHAUSEN, R.; CASTIÑEIRAS, D.; ESTEVE, V.; CLANCY, N.; REDONDO, J. I. A modified approach for the ultrasound-guided quadratus lumborum block in dogs: a cadaveric study. **Animals**, v. 11, n. 10, p. 2945, 2021. DOI: 10.3390/ani11102945.

WANG, Y.; WANG, X.; ZHANG, K. Effects of transversus abdominis plane block versus quadratus lumborum block on postoperative analgesia: a meta-analysis of randomized controlled trials. **BMC Anesthesiology**, v. 20, art. 103, 2020. DOI: 10.1186/s12871-020-01000-2.

WATANABE, R.; BERTOLIZIO, G.; CRUZ BENEDETTI, I.-C.; GARBIN, M. Perioperative analgesic management using bilateral ultrasound-guided lateral quadratus lumborum block in a dog with extrahepatic biliary obstruction. **Canadian Veterinary Journal**, v. 65, n. 12, p. 1234-1240, 2024.

XU, M.; TANG, Y.; WANG, J.; YANG, J. Quadratus lumborum block for postoperative analgesia after cesarean delivery: a systematic review and meta-analysis. **International Journal of Obstetric Anesthesia**, v. 42, p. 87-98, 2020. DOI: 10.1016/j.ijoa.2020.02.005.

ZHANG, Q.; XU, J.; OU, M.; LANG, B. Evaluation of analgesic effects and safety of quadratus lumborum block in patients undergoing laparoscopic surgery: a meta-analysis of randomized controlled trials. **Minerva Anestesiologica**, v. 88, n. 1-2, p. 62-71, 2022. DOI: 10.23736/S0375-9393.21.15807-9.

ZOFF, A.; LABORDA-VIDAL, P.; MORTIER, J.; AMENGUAL, M.; RIOJA, E. Comparison of the spread of two different volumes of contrast medium when performing ultrasound-guided transversus abdominis plane injection in dog cadavers. **Journal of Small Animal Practice**, v. 58, n. 5, p. 269-275, 2017. DOI: 10.1111/jsap.12639.

SUPPLEMENTARY MATERIAL 1 – ANATOMICAL CHARACTERISTICS OBSERVED DURING DISSECTION

During the dissections comparing the IM and LL approaches, anatomical variations between L2, L3, and L4 were observed in 37 out of 116 dissected hemiabdomens (Figure 8). These included: connection between L2 and L3 (11), bifurcation of L3 (9), bifurcation of L2 (9), genitofemoral nerve formed by L3 and L4 (3), connection between L3 and L4 (3), and absence of L3 (2). During the dissections carried out for equation validation, a connection between L2 and L3, absence of L3, and a bifurcation of L2 were observed.

An intimate connection was observed between the ventral branch of the first lumbar spinal nerve (VBSN of L1) and the cranial abdominal artery and vein. The course of these vessels perforated the iliac fascia on the ventral surface of the psoas muscle group. After the VBSN branched, it curved from a ventral to lateral direction and followed the aforementioned vessels during their intrafascial path (Figure 9). Divisions of these vessels were also observed, with a trajectory directly associated with the branches from T13 to L3 (Figure 10). These structures crossed the transversalis fascia together and were destined to supply or innervate the corresponding dermatomes (Figure 11). This pathway was consistently observed in all dissections, as previously described in the literature (Hermanson et al. 2020b).

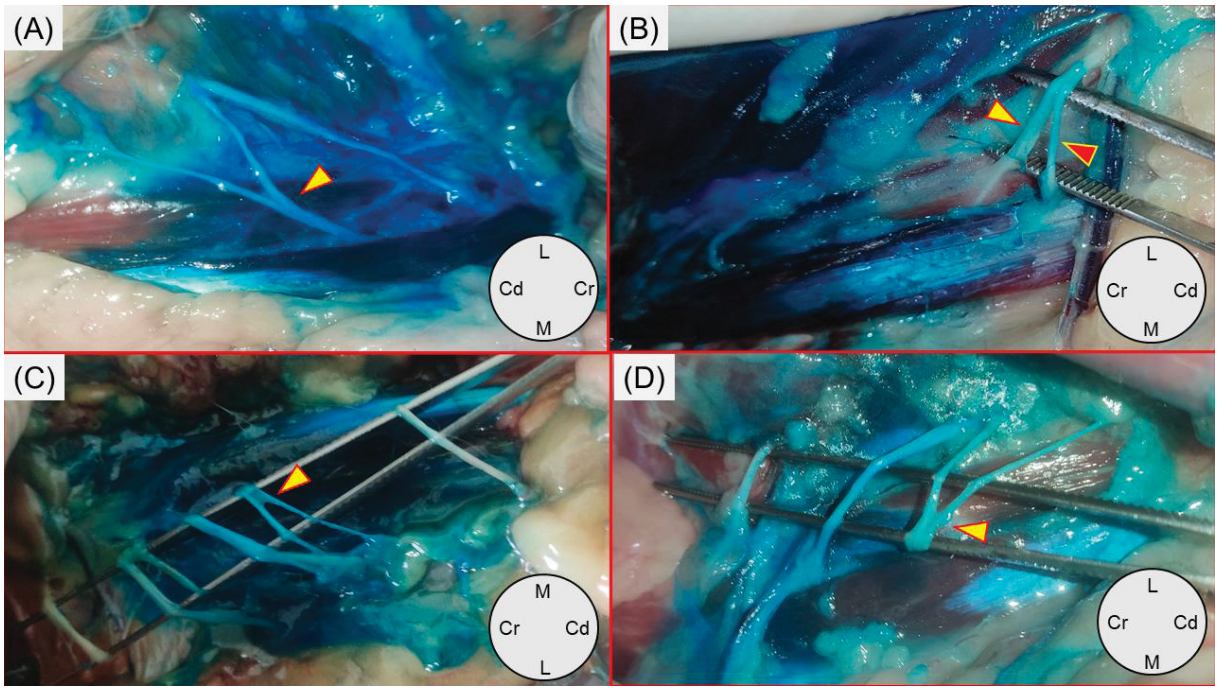

Figure 8. Anatomical characteristics in the ventral branches of the thoracolumbar spinal nerves observed during the dissection of canine cadavers to evaluate dye spread through the thoracolumbar fascia following quadratus lumborum block. (A) Bifurcation of L3 (yellow arrow) and connection with L2; (B) Connection between L3 (yellow arrow) and L4 (red arrow), with the deep circumflex iliac vein visible beneath the forceps; (C) Bifurcation of L3 (yellow arrow); (D) Bifurcation of L2 (yellow arrow).

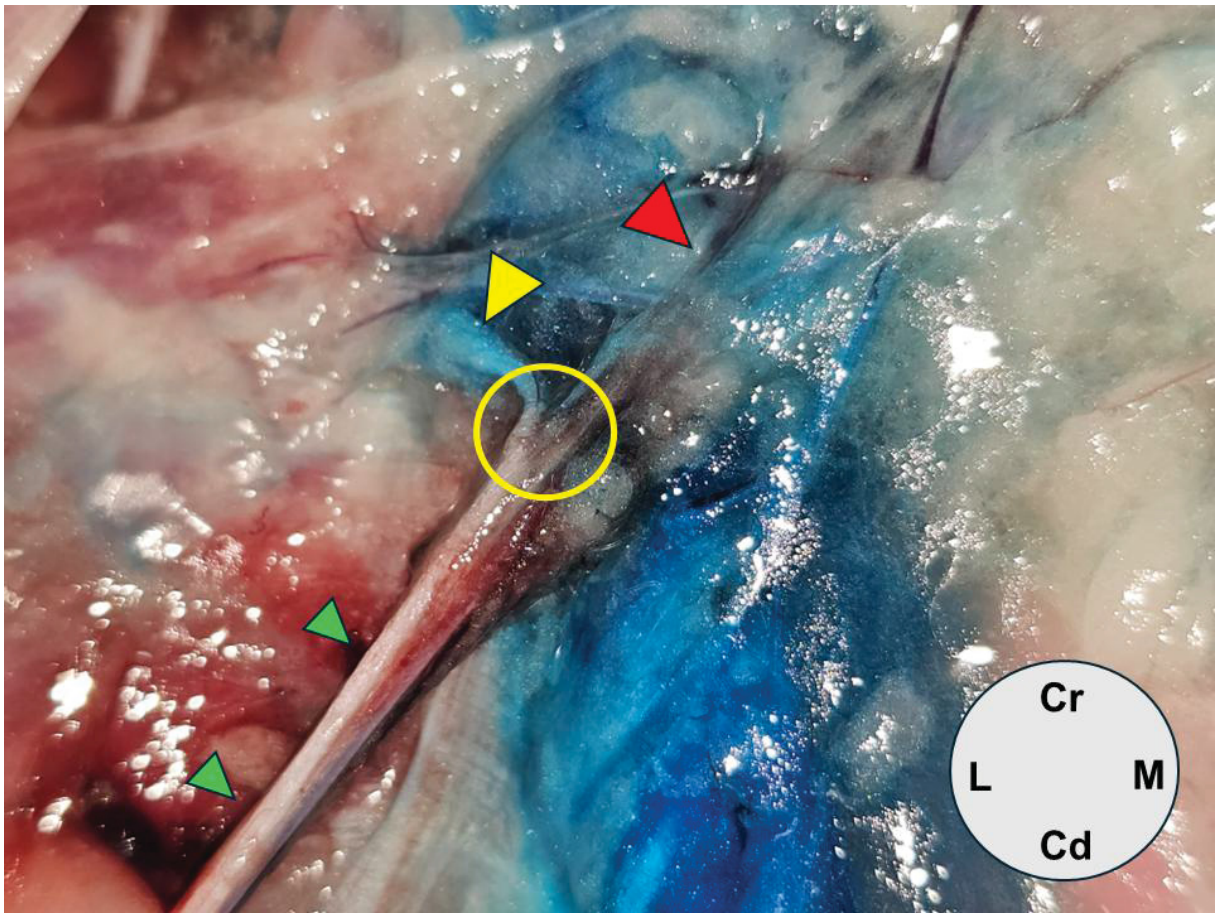

Figure 9. Pathway traveled by the ventral branch of the nerve from the first lumbar vertebra (VBSN-L1), after division into dorsal and ventral branches, along with the cranial abdominal artery and its satellite vein. *Note (yellow arrowhead) the proximal portion of the VBSN curving ventrolaterally to join (yellow circle) the abdominal artery (red arrowhead), and then continuing its course through the thoracolumbar fascia, lateral to the QL and psoas muscle group (green arrowhead).

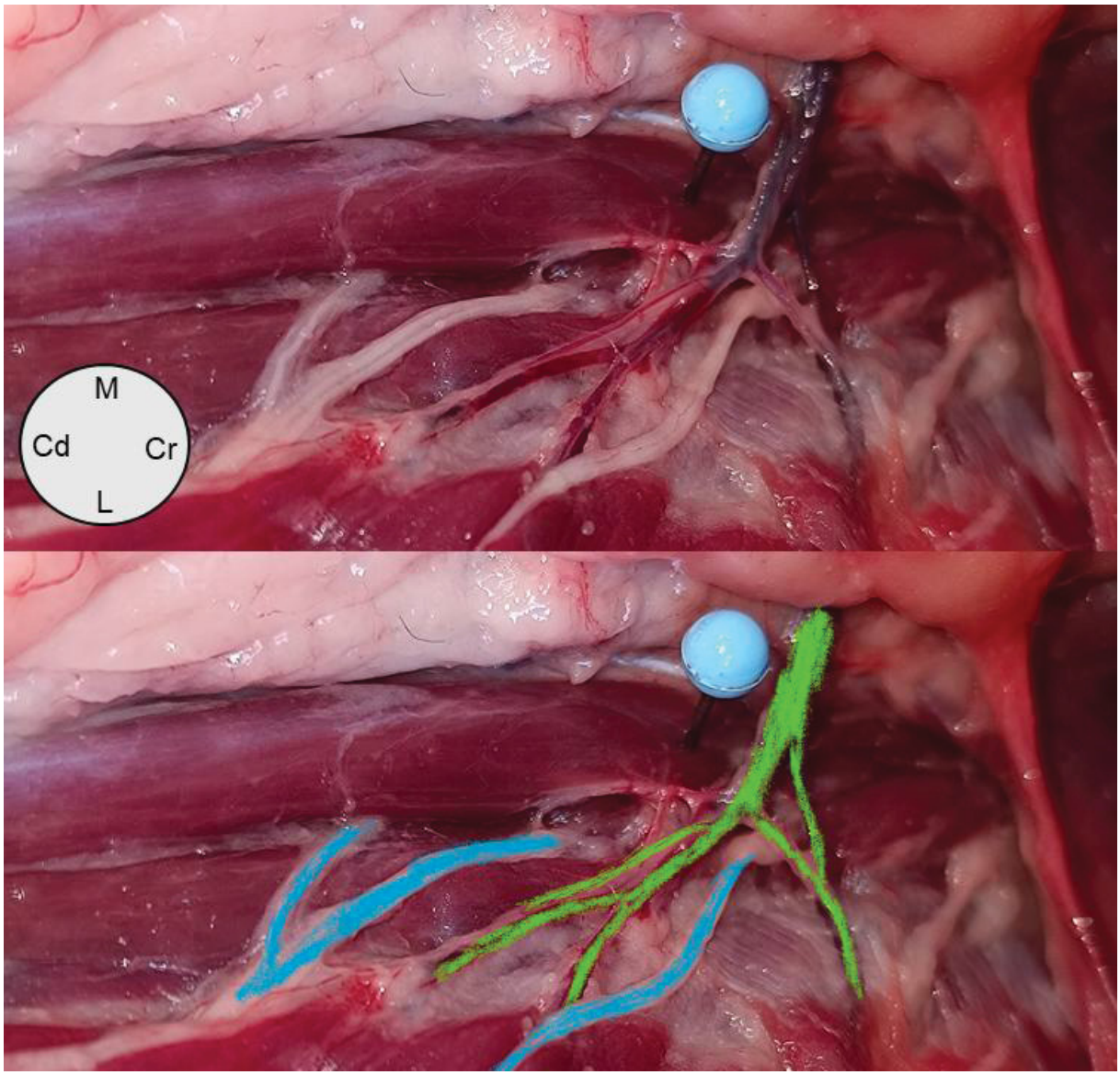

Figure 10. Cranial abdominal artery and vein (in green) following their course through the thoracolumbar fascia, displaying branches that accompany the paths of thoracolumbar nerves from T13 to L3 (in blue). *The blue pin represents the final needle placement site in the IM approach.

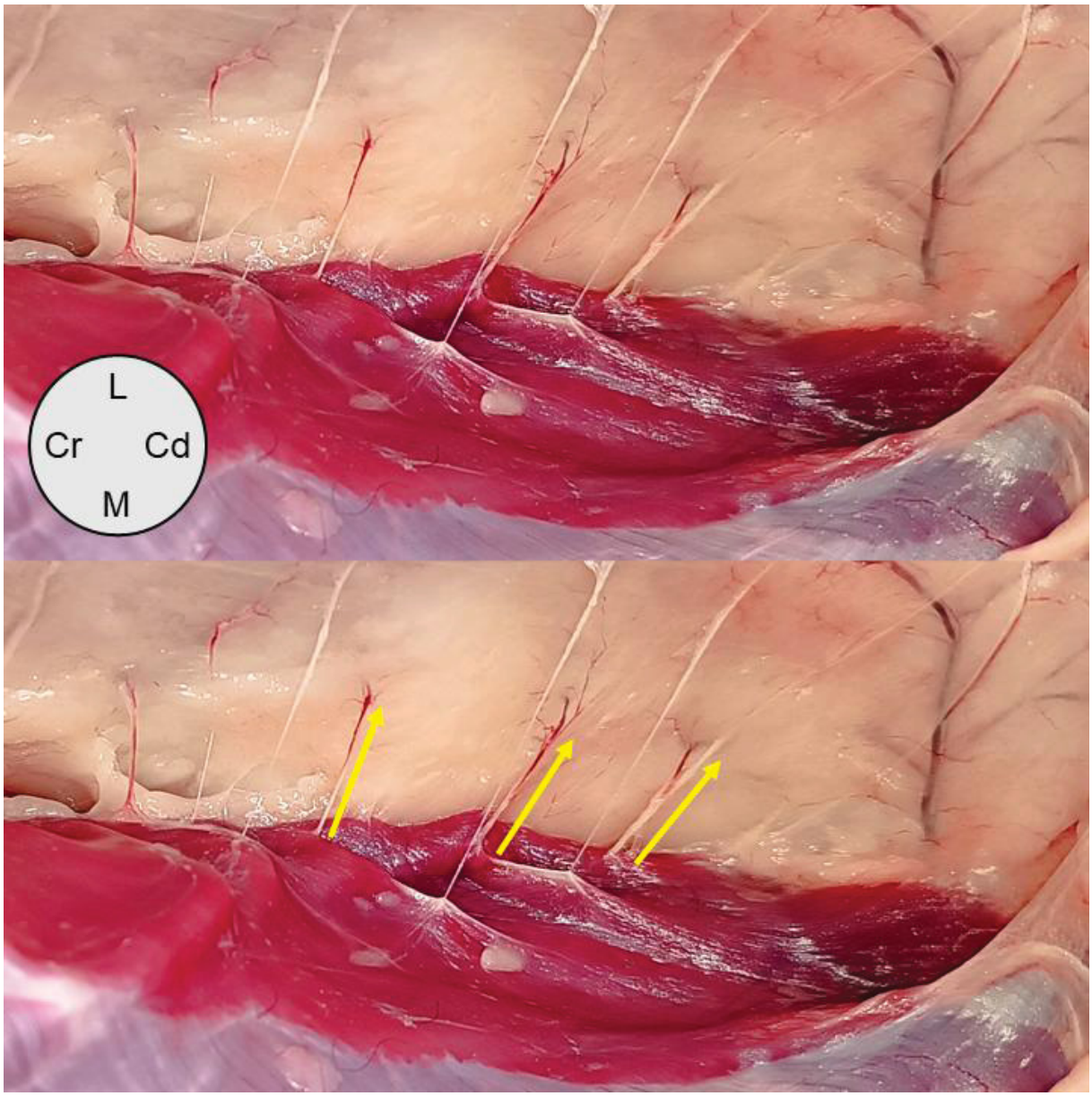

Figure 11. View of the subcutaneous region of a dissected canine cadaver. The yellow arrows indicate the course of the thoracolumbar nerves from L1 to L3 as they form their respective dermatomes. An intimate association with blood vessels originating from the cranial abdominal artery and vein can be observed.

SUPPLEMENTARY MATERIAL 2 – IMAGES OF CATHETER PASSAGE IN THE QLP OF DOG

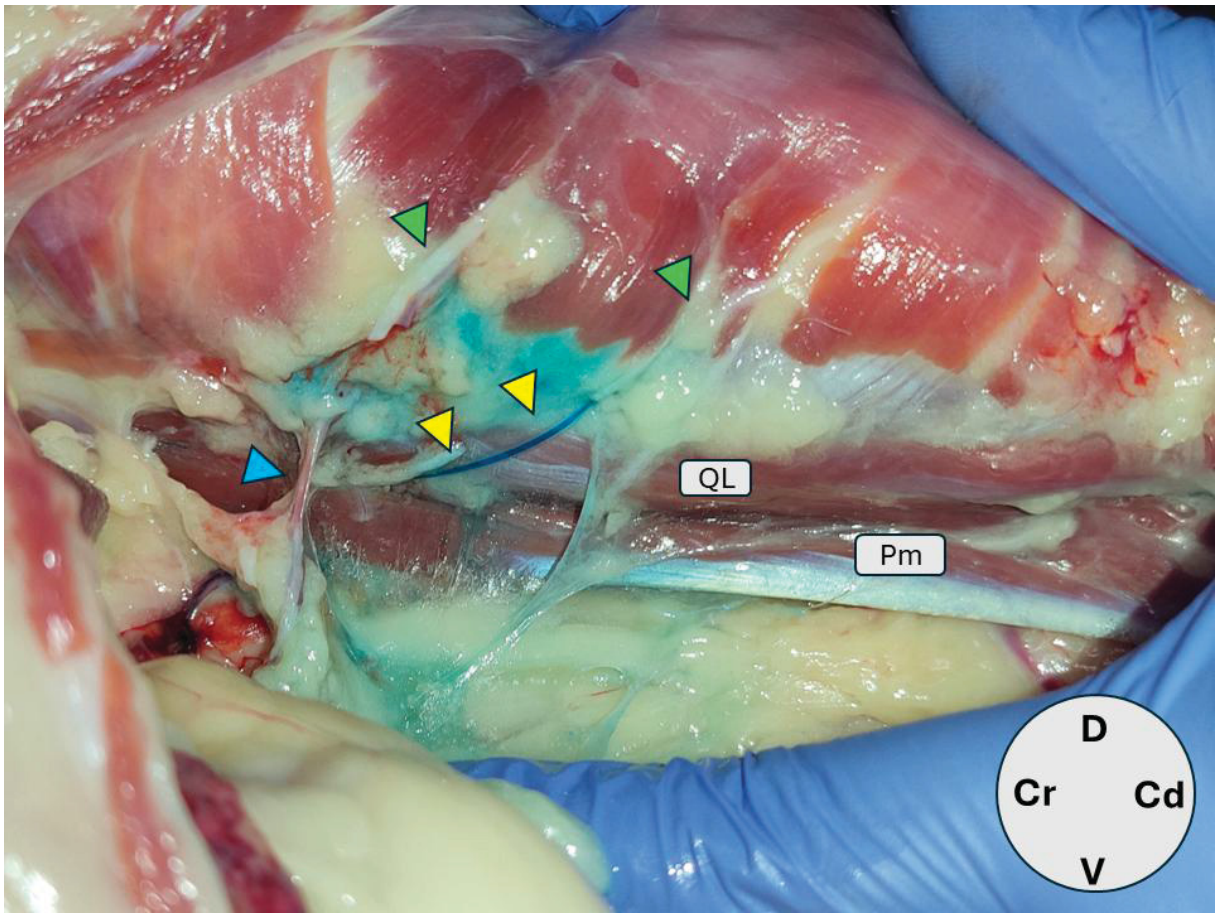

Figure 12. Visualization of the Quadratus Lumborum Plane (QLP) after dissecting the transversalis fascia through the retroperitoneum and removing excess fat in the left hemiabdomen of a canine cadaver with a body condition score of 4 (on a scale of 1–9), using a ventrolateral approach to the abdominal cavity. Yellow arrowhead: epidural catheter (Portex Epidural Catheter, Smiths Medical, Czech Republic) piercing the thoracolumbar fascia and positioned in the QLP using an intermuscular approach; QL, quadratus lumborum muscle; Pm, psoas minor muscle; Green arrowhead: ventral branches of the thoracolumbar nerves; Red arrow blue: cranial abdominal artery and vein.

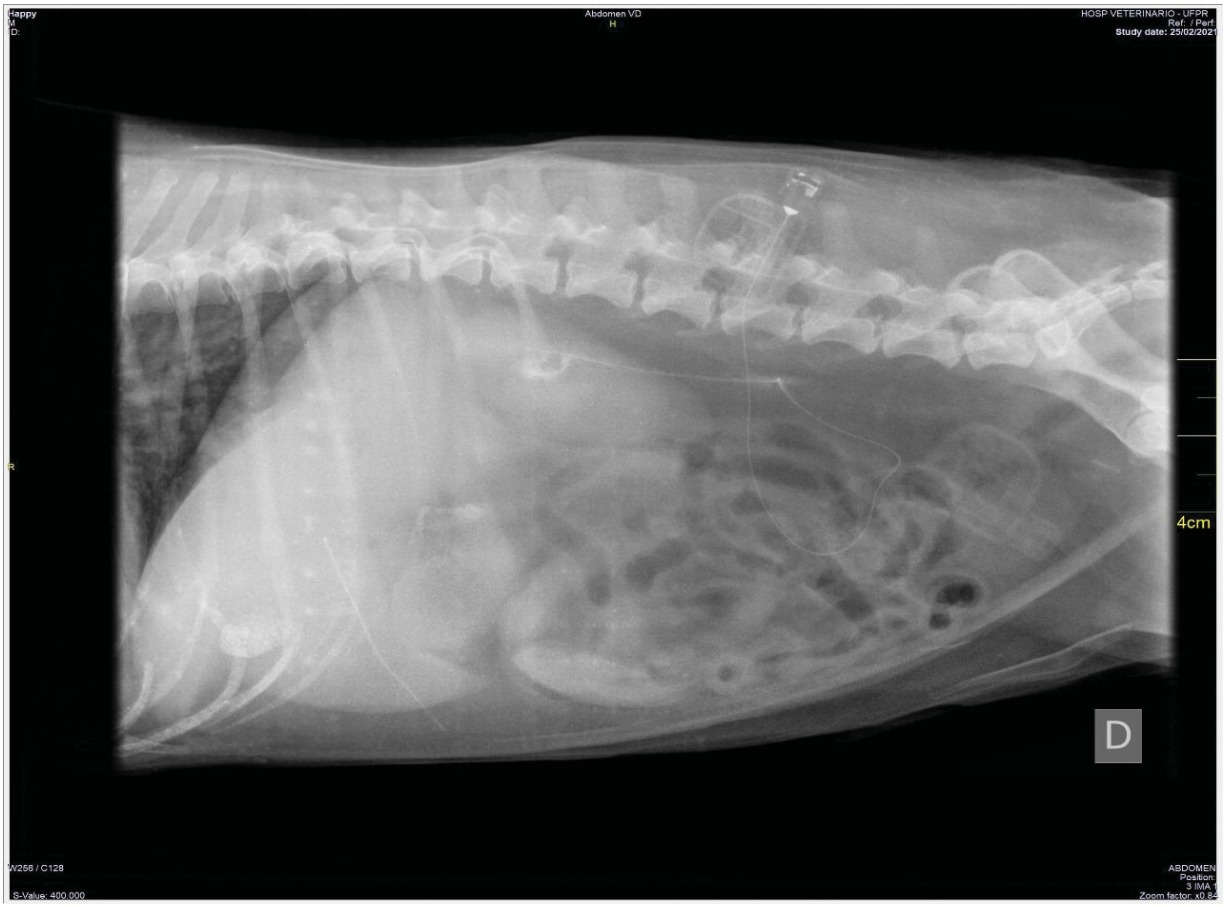

Figure 13. Radiograph of the thoracolumbar region of a dog positioned in right lateral recumbency. The presence of an epidural catheter (Portex Epidural Catheter, Smiths Medical, Czech Republic) is noted in the hypoaxial region of the lumbar spine, filled with iodinated contrast (Iomeron®, Bracco Imaging, Italy), in a caudocranial direction.

-

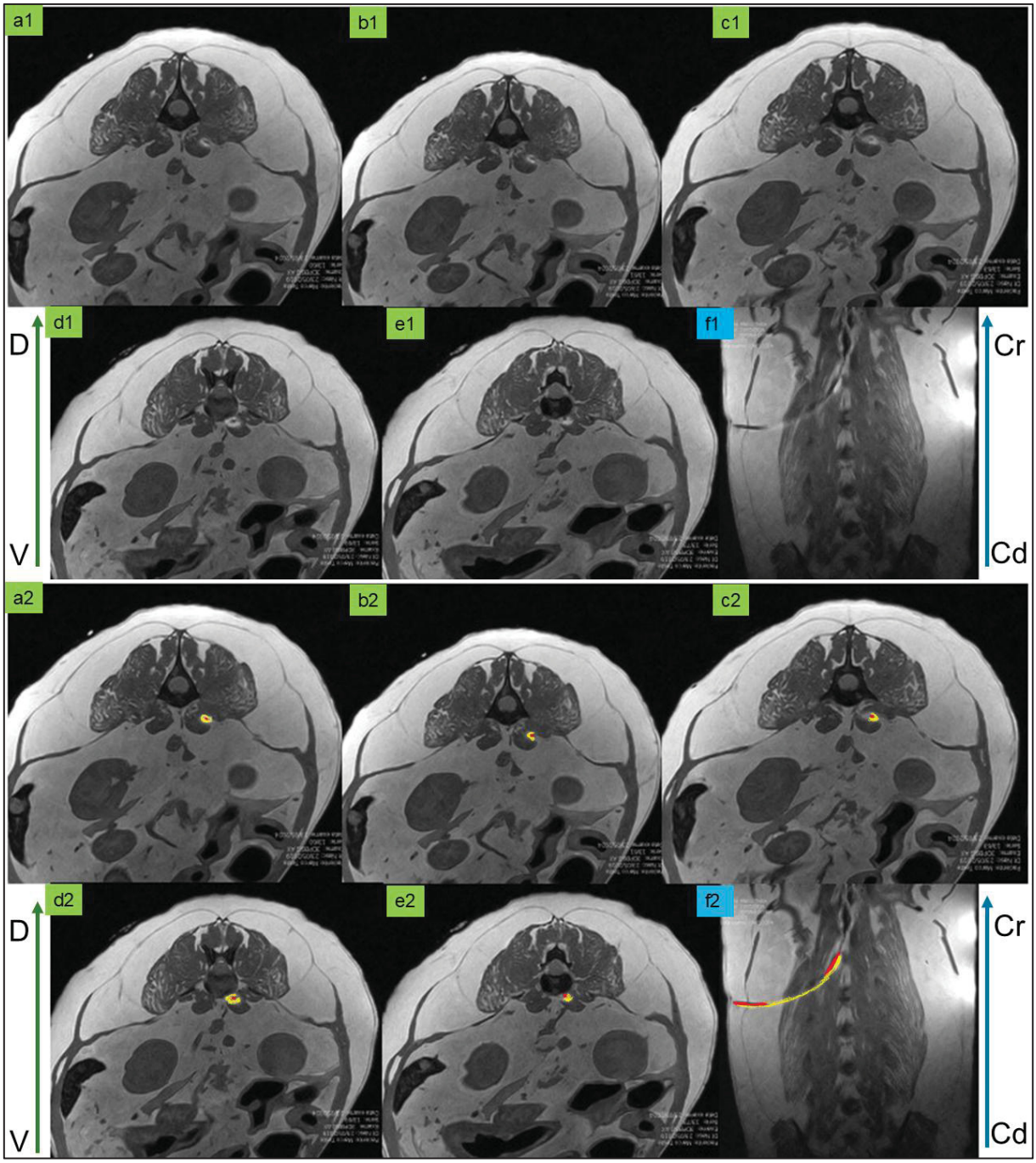

Figure 14. Axial plane magnetic resonance imaging (MRI) series of a canine cadaver acquired after the passage of an epidural catheter (Portex Epidural Catheter, Smiths Medical, Czech Republic) into the quadratus lumborum plane (QLP). Green images (a), (b), (c), (d), and (e) show transverse sections of the lumbar region (L1–L2), and blue image (f) shows a sagittal reconstruction, demonstrating the catheter trajectory along the QLP: (a1 – mid third of L2; b1 – cranial third of L2; c1 – caudal third of L1; d1 – mid third of L1; and e1 – cranial third of L1). Images (2) highlight the spread of the contrast medium (yellow shading) and the catheter path (red dots) along the intermuscular plane, piercing the thoracolumbar fascia near the L3 vertebral body and projecting in a caudocranial and lateromedial direction until reaching the L1 vertebral body.

SUPPLEMENTARY MATERIAL 3 – TABLES OF THE CADAVERIC STUDY ON QLP APPROACHES

Table 1. Morphometric characteristics (weight, body condition score*, spine length, thoracic and abdominal circumference) and ultrasound image quality (Quality-I) during the injection of a 0.1% methylene blue solution at volumes of 0.15, 0.3, and 0.6 mL·kg^{-1} in the quadratus lumborum plane, using either the intermuscular (IM) or lateral lumbar (LL) approach, in canine cadavers classified as small (S), medium (M), or large (G).

Cadaver size								
Size	Weight (kg)	Body Condition Score	Length (cm)			Quality-I		
			Spine	Thoracic	Abdome	Visualization of QLP structures	Needle projection visibility	Visibility of injected solution
S	6.6 (±2.2)	5 (iqr 2,7)	47.5 (±7.2)	42.6 (±6.2)	36.4 (±7.6)	2 (iqr 1)	2 (iqr 1)	1 (iqr 1)
M	14 (±2.9)	5 (iqr 3)	59.1 (±8.6)	55.2 (±6.7)	48.9 (±7.3)	2 (iqr 0.75)	2 (iqr 1)	2 (iqr 1)
L	26.7 (±7.2)	5 (iqr 3)	73.1 (±8.6)	72.5 (±9.6)	66.2 (±12.8)	2 (iqr 0.75)	2 (iqr 1)	1 (iqr 1)
Approach								
Approach	Weight (kg)	Body Condition Score	Length (cm)			Quality-I		
			Spine	Thoracic	Abdome	Visualization of QLP structures	Needle projection visibility	Visibility of injected solution
IM	15.1 (±8.1)	5 (iqr 3)	59.9 (±13.1)	56.1 (±11.4)	50.4 (±12.0)	2 (iqr 1)	2 (iqr 1)	2 (iqr 1)
LL	16.4 (±10.9)	5 (iqr 2)	60.3 (±13.5)	57.1 (±16.7)	50.6 (±18.5)	2 (iqr 0)	2 (iqr 1)	1.5 (iqr 1)
Approach/volume injected								
Group	Weight (kg)	Body Condition Score	Length (cm)			Quality-I		
			Spine	Thoracic	Abdome	Visualization of QLP structures	Needle projection visibility	Visibility of injected solution
IM0.15	16.3 (±10.2)	5 (iqr 2)	59.5 (±14.3)	57.7 (±13.1)	51.4 (±13.5)	2 (iqr 1)	2 (iqr 1)	2 (iqr 1)
IM0.3	15 (±7.3)	5 (iqr 3.5)	59.2 (±13.6)	55.2 (±10.8)	50.9 (±12.2)	2 (iqr 1)	2 (iqr 1)	1 (iqr 1)
IM0.6	14.4 (±6.7)	5 (iqr 3)	59.6 (±12)	55.2 (±10.8)	48.9 (±10.8)	2 (iqr 1)	2 (iqr 1)	2 (iqr 1)
LL0.15	15 (±8.5)	5 (iqr 2)	59.3 (±11.4)	54.1 (±12.8)	47.7 (±13.2)	2 (iqr 0.25)	2 (iqr 1)	1 (iqr 1)
LL0.3	17.8 (±12.6)	5 (iqr 3.25)	60.9 (±15.1)	59.7 (±18.6)	53.1 (±21.3)	2 (iqr 0.25)	2 (iqr 0.25)	2 (iqr 1)
LL0.6	16.3 (±11.6)	5 (iqr 2.25)	60.7 (±14.5)	57.4 (±18.4)	50.8 (±20.5)	2 (iqr 0.25)	2 (iqr 1)	2 (iqr 1)

Analyzed for normality of distribution using the Shapiro-Wilk test ($p < 0.05$). Mean values with standard deviation for normally distributed data and median with interquartile range for non-normally distributed data.
* WSAVA nutrition guidelines (Freeman et al., 2011)

Table 2. Results of the two-way ANOVA analysis for craniocaudal spread, dorsoventral spread, and number of stained nerves for the quadratus lumborum plane injection technique in canine cadavers, related to the volumes of 0.15, 0.3, and 0.6 mL kg^{-1}, the intermuscular or lateral lumbar approaches, and the interaction between volume and approach.

	p-values associated		
Source of variation	**Cranio-caudal spread**	**Dorsalventral spread**	**Number of stained nerves**
Volume	< 0.001*	0.008*	< 0.001*
Approach	0.7664	0.028*	0.4457
Interaction (Volume x Approach)	0.9867	0.7653	0.6755

* Significant values.

SUPPLEMENTARY MATERIAL 4 – IMAGES OF THE CADAVERIC STUDY ON QLP APPROACHES.

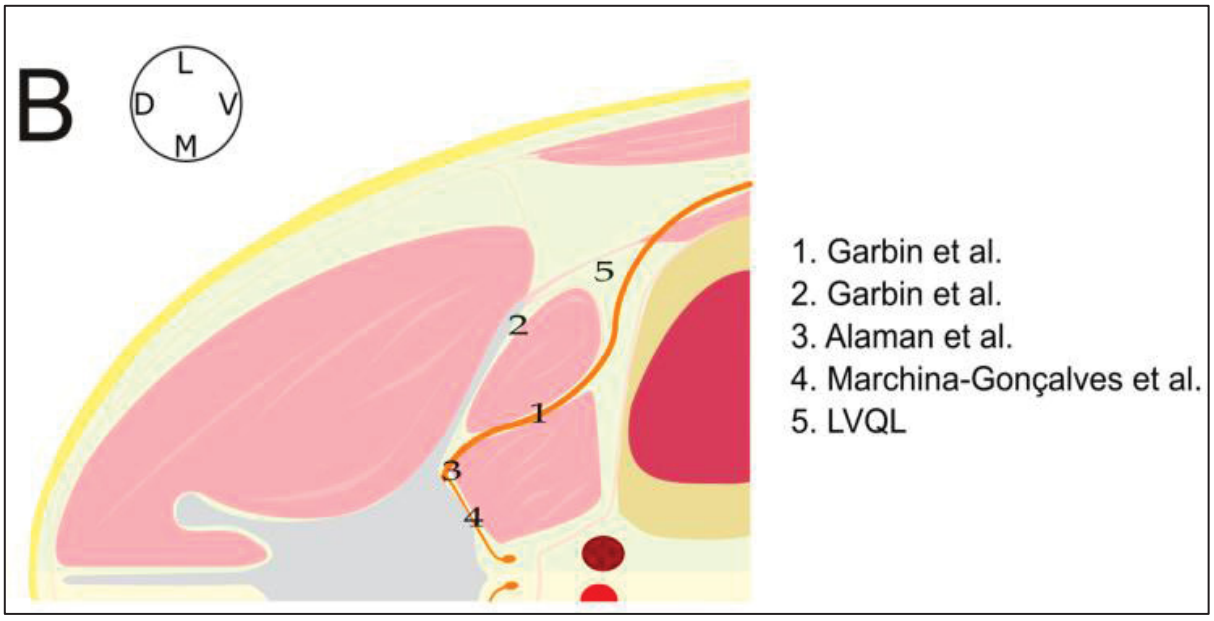

Figure 15. (B) Schematic illustration of the anatomy at the level of the first lumbar vertebra in a dog positioned in lateral recumbency, showing the needle placement sites described in cadaveric studies for performing the quadratus lumborum block, numbered accordingly (Marchina-Gonçalves et al. 2023).

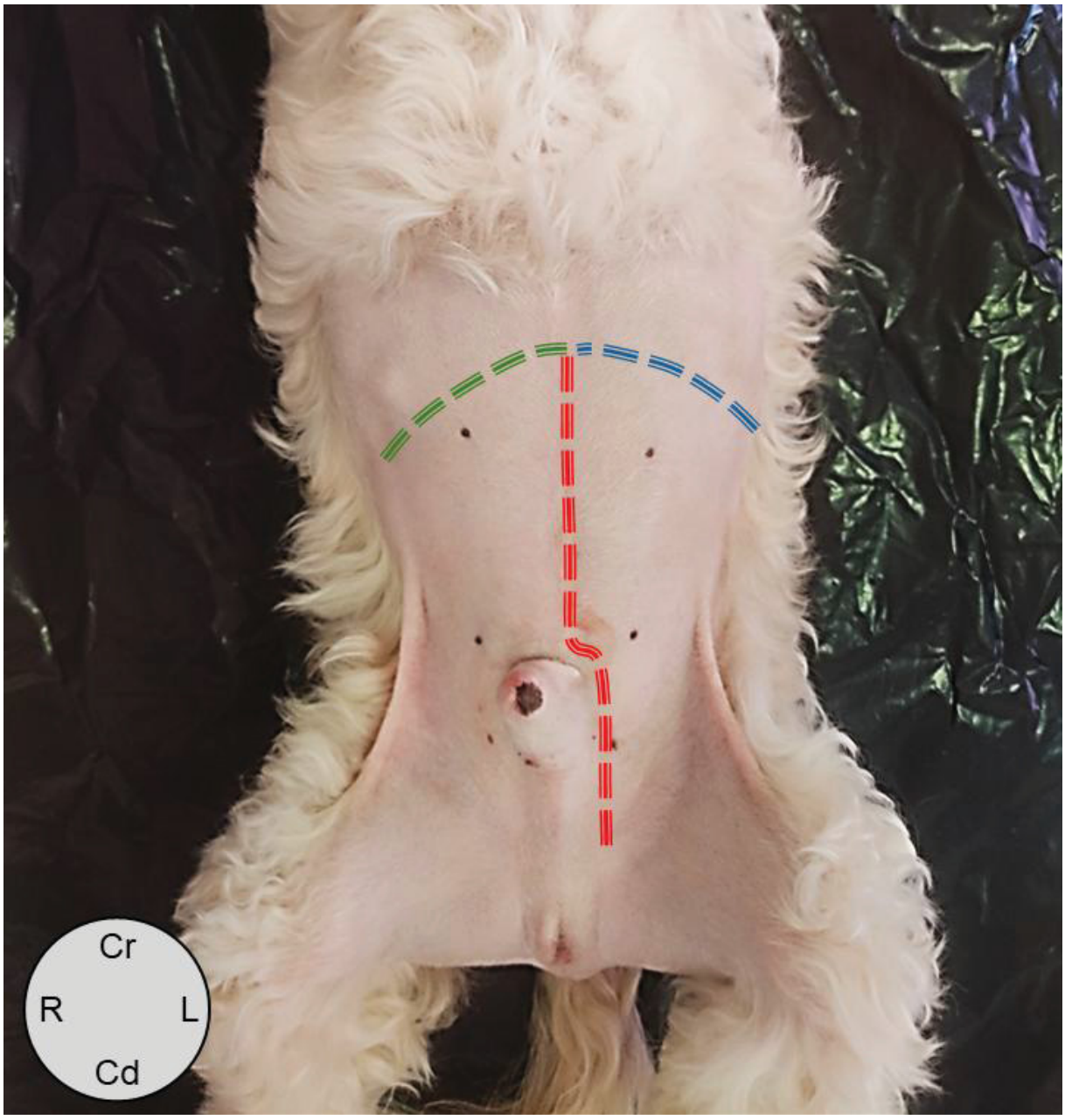

Figure 16. Ventral view of the abdomen of a canine cadaver positioned in dorsal recumbency with the incisions made to expose the ventrolateral abdominoventral retroperitoneum. The red dashed line indicates the first incision made along the ventral midline (from the xiphoid to the pubis), the blue dashed line indicates the second incision made parallel to the caudal edge of the left costal arch (immediately after the midline incision), and the green dashed line indicates the third incision made parallel to the caudal edge of the right costal arch (after dissection of the left retroperitoneum).

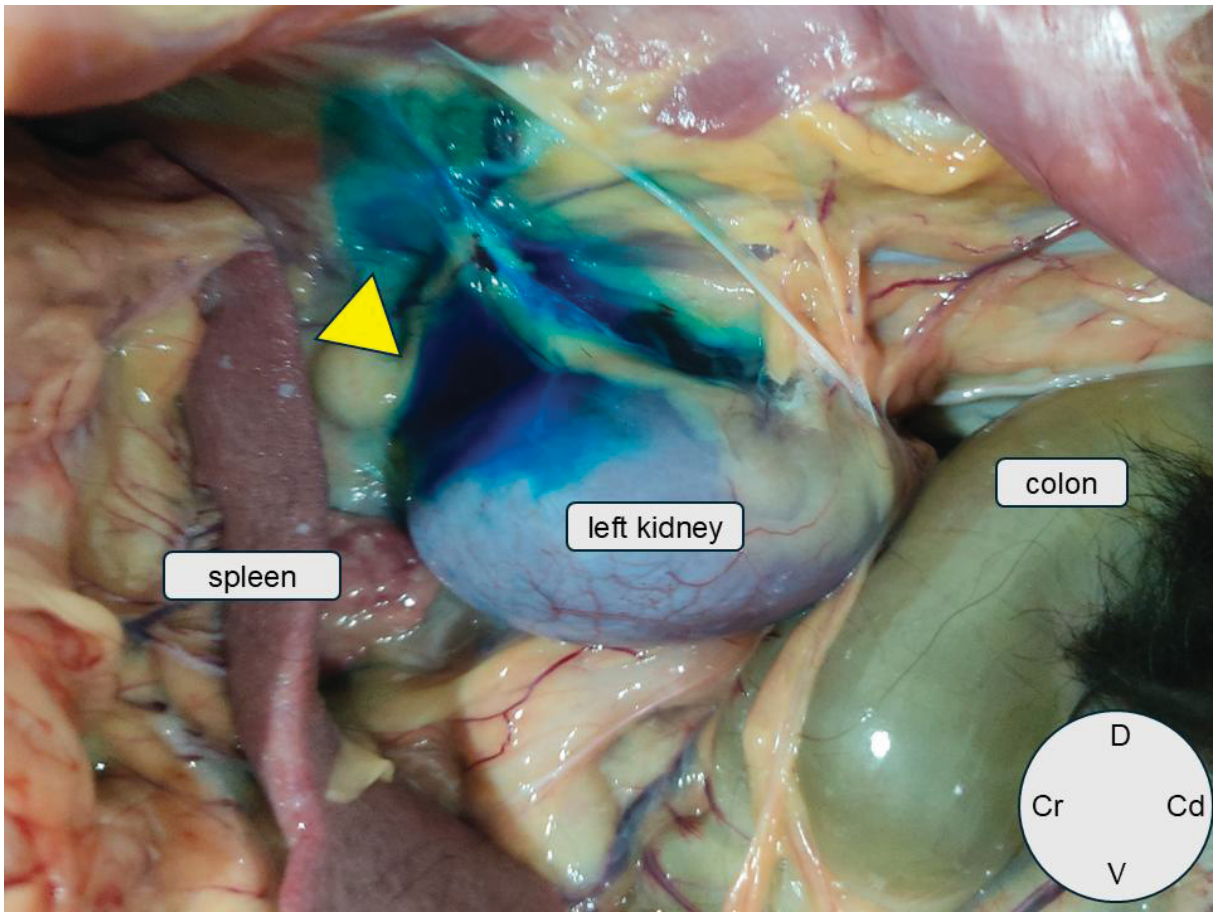

Figure 17. Visualization of the Quadratus Lumborum Plane (QLP) after dissecting the transversalis fascia through the retroperitoneum and removing excess fat in the left hemiabdomen of a canine cadaver with a body condition score of 1 (on a scale of 1–9), using a ventrolateral approach to the abdominal cavity. Yellow arrowhead: abnormal spread of the dye solution (methylene blue) into the transversalis fascia (retroperitoneal space).